DMD Fast Forward. Published on August 5, 2020 as DOI: 10.1124/dmd.120.000064
This article has not been copyedited and formatted. The final version may differ from this version.

Comparison of In Vitro to In Vivo Extrapolation Approaches for Predicting Transporter-Mediated Hepatic Uptake Clearance Using Suspended Rat Hepatocytes

Na Li, Akshay Badrinarayanan, Xingwen Li, John Roberts, Mike Hayashi, Manpreet Virk,

Anshul Gupta*

Department of Pharmacokinetics and Drug Metabolism, Amgen Research, Amgen Inc. Cambridge, MA 02142

DMD Fast Forward. Published on August 5, 2020 as DOI: 10.1124/dmd.120.000064
This article has not been copyedited and formatted. The final version may differ from this version.

Running Title: Prediction of transporter-mediated hepatic uptake CL in rat

*Corresponding Author: Anshul Gupta

Address: Department of Pharmacokinetics and Drug Metabolism, Amgen Research, Amgen Inc.

360 Binney St., Cambridge, MA 02142

Phone: +1 (617) 444 5205

Email: agupta.pharmaceuticals@gmail.com

The number of text pages: 40

The number of tables: 5

The number of figures: 2

The number of references: 41

The number of words in the Abstract: 219

The number of words in the Introduction: 787

The number of words in the Discussion: 1502

DMD Fast Forward. Published on August 5, 2020 as DOI: 10.1124/dmd.120.000064
This article has not been copyedited and formatted. The final version may differ from this version.

Abbreviations

AAFE, absolute average fold error;

BSA, bovine serum albumin;

CL_H, systemic plasma clearance mediated by hepatic elimination;

CL_{int}, hepatic intrinsic clearance;

$CL_{int,met}$, intrinsic hepatic metabolic clearances;

CYP, cytochrome P450;

$f_{u,p}$, the unbound fraction in rat plasma;

$f_{u,hep}$, the unbound fraction in hepatocyte suspension incubation;

$f_{u,liver\ tissue}$, the unbound fraction in rat liver tissue;

$f_{u,KHB\ w\ 4\%,BSA}$, unbound fraction in KHB buffer containing 4% BSA;

IVIVC, in vitro to-in vivo correlation;

IVIVE, in vitro-to-in vivo extrapolation;

Kp, hepatocytes to media partition coefficient at steady state;

$Kp_{uu,ss}$, unbound hepatocytes to media partitioning coefficient at steady-state;

LC-MS/MS, liquid chromatography– tandem mass spectrometry;

OATP, organic anion-transporting polypeptide;

PS_{inf}, hepatic uptake clearance for total drug;

$PS_{inf,act}$, hepatic active uptake clearance for total drug;

$PS_{inf,dif}$, passive influx for total drug;

$PS_{u,inf}$, unbound hepatic uptake clearance;

PK, pharmacokinetics;

RMSLE, root mean squared logarithmic error

DMD Fast Forward. Published on August 5, 2020 as DOI: 10.1124/dmd.120.000064
This article has not been copyedited and formatted. The final version may differ from this version.

Abstract

Clearance (CL) prediction remains a significant challenge in drug discovery, especially when complex processes such as drug transporters are involved. The present work explores various in vitro to in vivo extrapolation (IVIVE) approaches to predict hepatic CL driven by uptake transporters in rat. Broadly, two different IVIVE methods using suspended rat hepatocytes were compared: initial uptake CL ($PS_{u,inf}$) and intrinsic metabolic CL ($CL_{int,met}$) corrected by unbound hepatocytes to media partition coefficient (Kp_{uu}). Kp_{uu} was determined by temperature method (Temp $Kp_{uu,ss}$), homogenization method (Hom $Kp_{uu,ss}$), and initial rate method ($Kp_{uu,V0}$). In addition, impact of albumin (BSA) on each of these methods was investigated. Twelve compounds, which are known substrates of organic anion-transporting polypeptides (OATP) representing diverse chemical matter, were selected for these studies. As expected, $CL_{int,met}$ alone significantly underestimated hepatic CL for all the test compounds. Overall, predicted hepatic CL using $PS_{u,inf}$ with BSA, Hom $Kp_{uu,ss}$ with BSA and Temp $Kp_{uu,ss}$ showed the most robust correlation with in vivo rat hepatic CL. Adding BSA improved hepatic CL prediction for selected compounds when using $PS_{u,inf}$ and Hom $Kp_{uu,ss}$ methods, with minimal impact on Temp $Kp_{uu,ss}$ and $Kp_{uu,V0}$ methods. None of the IVIVE approaches required empirical scaling factor. These results suggest that supplementing rat hepatocyte suspension with BSA may be essential in discovery research for novel chemical matters to improve CL prediction.

DMD Fast Forward. Published on August 5, 2020 as DOI: 10.1124/dmd.120.000064
This article has not been copyedited and formatted. The final version may differ from this version.

Significance Statement

The current investigation demonstrates that hepatocyte uptake assay supplemented with 4% BSA is a valuable tool for estimating unbound hepatic uptake CL and Kp_{uu}. Based upon extended clearance concept, direct extrapolation from these in vitro parameters significantly improved the overall prediction of hepatic CL for OATP substrates in rat. This study provides a practical IVIVE strategy for predicting transporter-mediated hepatic CL in early drug discovery.

DMD Fast Forward. Published on August 5, 2020 as DOI: 10.1124/dmd.120.000064
This article has not been copyedited and formatted. The final version may differ from this version.

Introduction

Prediction of human pharmacokinetics (PK) of drug candidates is one of the major focus during drug discovery to reduce attrition during clinical development. Liver is the major organ responsible for drug disposition and elimination. Upon active uptake or passive diffusion from blood into hepatocytes, drugs undergo metabolism and biliary excretion. Therefore, quantitative prediction of hepatic CL is an essential step towards accurately predicting human PK. Although allometric scaling across preclinical species has been commonly used for human PK prediction in drug discovery, mechanism driven IVIVE is the more preferred approach to predict hepatic CL because of the species difference in the function and/or expression of drug metabolizing enzymes and transporters in liver. When metabolism is the predominant CL mechanism, liver microsome or hepatocytes have served as an essential tool for predicting hepatic CL (Kilford et al. 2009, Hallifax et al. 2010, Di et al. 2012). However, when transporters are involved in drug disposition and elimination, the in vitro and in vivo correlation (IVIVC) and human PK prediction become highly uncertain (Shitara et al. 2013). Particularly, when hepatic uptake is the rate determining step for hepatic CL, direct extrapolation from intrinsic metabolic CL significantly underestimates the drug CL observed in vivo. Due to the difference between the in vitro and in vivo systems (e.g. transporter expression level, activity, static vs dynamic), the empirical scaling factor has been proposed to optimize the prediction of hepatic uptake CL (Jones et al. 2012, Li et al. 2014). Empirical scaling factor has been found to be system- and compound-dependent, thus presenting a great challenge to implement this approach in supporting drug discovery efforts.

DMD Fast Forward. Published on August 5, 2020 as DOI: 10.1124/dmd.120.000064
This article has not been copyedited and formatted. The final version may differ from this version.

Quantitative IVIVE approaches have been demonstrated to predict the hepatic CL from uptake CL obtained in human cryopreserved hepatocytes, although these examples are limited to only a few organic anions (Watanabe et al. 2010, Watanabe et al. 2011). Based upon the extended clearance concept, Izumi et al. demonstrated improved IVIVE for a variety of drugs by correcting intrinsic metabolic CL with Kp_{uu} (Izumi et al. 2017). However, for the highly bound compounds, the application of these IVIVE approaches are still limited because of the experimental challenges for accurately determining hepatic uptake CL and Kp_{uu} because of the significant non-specific binding to the cell surface and experimental devices, and limited analytical sensitivity to accurately determine the unbound fraction in matrices.

Other than the difference of transporter expression level and activity, another deviation of in vitro systems from in vivo is that in vitro hepatic uptake assay often is carried out in a protein free condition, in contrast to the systemic circulation containing albumin. Primarily synthesized in liver, albumin is a key protein that maintains the oncotic pressure of blood and has been proven to be involved in drug metabolism and transport (Tessari 2003, Rabbani and Ahn 2019). For the highly bound compounds, the non-specific binding to the assay device and/or cell membrane surface could significantly contribute to the inaccuracy or underestimation of in vitro transport rate. The phenomenon of albumin-mediate hepatic uptake has been reported previously in various experimental systems (Tsao et al. 1988, Tsao et al. 1988). Recent studies have demonstrated that the unbound intrinsic hepatic uptake CL was enhanced by addition of bovine serum albumin (BSA) or human serum albumin (HSA), subsequently resulting in improvement in the prediction of the hepatic uptake CL of OATP substrates in rat/human hepatocyte suspension (Miyauchi et al. 2018, Kim et al. 2019).

DMD Fast Forward. Published on August 5, 2020 as DOI: 10.1124/dmd.120.000064
This article has not been copyedited and formatted. The final version may differ from this version.

A robust mechanism-driven IVIVE strategy is pivotal for building confidence in human PK prediction in order to prioritize compounds during drug discovery phase. Rodent is the most commonly used preclinical species for assessing pharmacokinetics and pharmacodynamic in early stages of drug discovery. In the present study, we aimed at identifying the most reliable and practical in vitro approach to establish good IVIVC in rat. The twelve OATP substrates with diverse physicochemical properties, were selected for this investigation. For most of the compounds, OATP1B1 is the dominant uptake transporter responsible for the hepatic uptake, except telmisartan which is only transported by OATP1B3 (**Supplemental Table S1**). The hepatic uptake has been proven to be the rate-determining step for hepatic CL for these compounds, as indicated by preclinical and clinical evidence (**Supplemental Table S1**). In addition, uptake in rat hepatocyte in the absence and presence of 4% BSA was conducted to investigate the impact of albumin on intrinsic hepatic uptake CL ($PS_{u,inf}$) and Kp_{uu} estimation. Subsequently, these in vitro parameters were utilized to predict hepatic CL via two advanced IVIVE approaches, 1) directly predicting the hepatic CL using the initial uptake CL determined in rat hepatocytes suspension in the absence or presence of 4% BSA; 2) prediction based on intrinsic metabolic CL with correction of the Kp_{uu} according to the extended clearance concept.

DMD Fast Forward. Published on August 5, 2020 as DOI: 10.1124/dmd.120.000064
This article has not been copyedited and formatted. The final version may differ from this version.

Materials and Methods

Chemicals and Reagents

Rosuvastatin calcium, atorvastatin calcium, pravastatin sodium, pitavastatin calcium, glyburide, valsartan, and telmisartan were purchased from MilliporeSigma (St. Louis, MO). Fluvastatin sodium and cerivastatin were purchased from Tocris bioscience (Bristol, UK). Bosentan was purchased from Bosche Scientific (New Brunswich, NJ). Asunaprevir was obtained from Advanced ChemBlock Inc (Burlingame, CA) and nateglinide was obtained from Tokyo Chemical Industry Co, Ltd (TCI) (Tokyo, Japan). Rifamycin SV sodium salt was purchase from MP Biomedicals, LLC (Solon, OH). Cryopreserved rat hepatocytes (lot JTJ), Krebs-Henseleit buffer (KHB), pooled rat plasma and rat liver homogenates were purchased from Bioreclamation IVT, LLC (Hicksville, NY). The cryopreserved hepatocytes thawing media (CHRM®) was obtained from APSciences, Inc (APS) (Columbia, MD). Dulbecco's Modified Eagle Medium (DMEM) and L-glutamine were obtained from Thermo Fisher Scientific (Waltham, MA). Dimethyl sulfoxide and bovine serum albumin were purchased from MilliporeSigma (St. Louis, MO). HPLC grade acetonitrile and water were purchased from Burdick & Jackson (Muskegon, MI).

Permeability Determination

Transcellular permeability studies using MDCKII (Madin Darby Canine Kidney Epithelial Cells) cell monolayers were conducted at Q^2 Solutions (Indianapolis, IN). Briefly, transcellular assay was performed on day 4 post plating of the MDCKII cells on 96-well transwell plates. Cells were pre-incubated with assay buffer (HBSS, pH 7.4 supplemented with 10 mM Hepes, 1 µM

DMD Fast Forward. Published on August 5, 2020 as DOI: 10.1124/dmd.120.000064
This article has not been copyedited and formatted. The final version may differ from this version.

elacridar and 0.1% BSA) for 30 minutes. After pre-incubation, assay buffer containing 5 µM test compound was added into the apical compartment, and assay buffer alone was added to the basal compartment. Elacridar (1 µM) was added to assay buffer at all times to inhibit any endogenous P-gp activity. Each incubation was performed in triplicate. The plates were re-assembled and incubated (37°C, 5% CO_2) for two hours. At the end of incubation, samples from receiver and donor compartments were collected and analyzed by LC-MS/MS, and the apparent permeability coefficient (P_{app}) of tested compounds was calculated: $P_{AB} = (dQ / dt) / (A * C_0)$, where dQ / dt is the apical-to-basal penetration rate of the agent, A is the surface area of the cell monolayer on the transwell, and C_0 is the initial concentration of the test compound.

Determination of Unbound Fraction in Different Biological Matrices

The binding in rat plasma, rat liver tissue homogenate, KHB buffer containing 4% BSA and hepatocytes suspension was performed using ultracentrifugation method as previously described with slightly modification (Nakai et al. 2004). Rat liver homogenate was prepared as 1g tissue per 4 mL of phosphate-buffered saline (dilution factor = 5). Briefly, rat plasma, diluted liver tissue homogenate, KHB with 4% BSA were spiked with test article at concentration of 5 µM and hepatocyte suspension at concentration 0.5 µM. Thereafter, 25 µL aliquots of spiked matrix were transferred to a sample plate and kept on ice to represent total drug. 220 µL aliquots were transferred to ultracentrifuge tubes and spun at 190,000 x g for 4.5 hours in a Type 42.2 rotor (Beckman Coulter) at 37°C. The remainder of spiked plasma was incubated at 37°C for the duration of the centrifugation period to be used to evaluate stability of test article. After centrifugation, 25 µL aliquots of the aqueous supernatant representing unbound fractions and the stability control plasma were transferred to the sample plate respectively. Samples were matrix

DMD Fast Forward. Published on August 5, 2020 as DOI: 10.1124/dmd.120.000064
This article has not been copyedited and formatted. The final version may differ from this version.

matched and quenched with cold acetonitrile with 0.1% formic acid containing internal standard (1 µM tolbutamide). The samples were vortex-mixed and centrifuged at 3400 x g for 15 minutes at 4°C. The supernatants were analyzed by LC-MS using a Waters Acquity H-Class UPLC system with a BEH C18 column (1.7 um x 2.1 mm x 50 mm) connected to a Q Exactive™ Hybrid Quadrupole-Orbitrap™ Mass Spectrometer (Thermo Scientific™) in full scan positive mode. The unbound fraction in rat plasma ($f_{u,\ plasma}$) and KHB with 4% BSA ($f_{u,\ BSA}$) was calculated from the ratio of analyte detected in the aqueous layer after centrifugation relative to the total concentration in the original matrix. The fraction unbound in tissue homogenates was corrected for dilution according to the equation described in (Kalvass et al. 2007):

$$\text{Undiluted } f_u = \left(\frac{1/D}{\left(\left({}^{1}/_{f_u} \right) - 1 \right) + 1/\text{D}} \right) \qquad (1)$$

where undiluted f_u is the adjusted fraction unbound in tissue, f_u is the measured fraction unbound assuming no dilution, and D is the -fold dilution of the tissue.

Measurement of $CL_{int,met}$ by Using Cryopreserved Rat Hepatocytes

Intrinsic metabolic CL was determined using cryopreserved Sprague-Dawley rat hepatocytes in suspension (Lot # JTJ) in the standard 1 hr incubation assay. Cryopreserved rat hepatocytes were thawed and recovered in pre-warmed CHRM®. After a quick centrifugation at 100 g for 10 min, the cells were reconstituted in pre-warmed Dulbecco's Modified Eagle Medium (DMEM, Thermo Fisher Scientific) supplemented with 2 mM L-glutamine (Thermo Fisher Scientific). The hepatocytes with equal or greater than 80% viability were diluted to 0.5 x 10^6 cells/mL in pre-

DMD Fast Forward. Published on August 5, 2020 as DOI: 10.1124/dmd.120.000064
This article has not been copyedited and formatted. The final version may differ from this version.

warmed DMEM. The reaction was initiated by spiking test compounds into the hepatocyte suspension to achieve a final concentration of 0.5 µM and incubate at 37°C in a humidified CO_2 incubator for 1 hours on a thermomixer shaker. At 0, 10, 20, 30, 45 and 60 time points, the reaction was stopped by adding quench solution (acetonitrile with 0.1% formic acid with tolbutamide as internal standard). After centrifugation at 3750g for 45 min, the supernatants were analyzed for test compound and IS by RapidFire 365 high-throughput SPE system interfaced with a 6550 QTOF mass spectrometer (Agilent) (Supplement method). The apparent metabolic intrinsic clearance $CL_{int, met}$ (µL/min/10^6 cells) was determined based on the degradation half-life estimated from analyte to IS peak area ratio time profile data.

In vitro Uptake Assay in Rat Hepatocytes Suspension

Uptake assay were performed in cryopreserved rat hepatocytes in suspension using a centrifugal filtration method described previously (Hirano et al. 2004). Cryopreserved rat hepatocytes (Lot# JTJ) were thawed and recovered in pre-warmed CHRM®. After a quick centrifugation at 100 g for 10 min, the cells were reconstituted in iced-cold KHB in the absence or presence of 8% bovine serum albumin at cell density of 1.0 x 10^6 cells/mL. Hepatocytes with greater than 85% viability were used in all the uptake study described below. The cells (2X of final concentration) were aliquoted into glass tube and stored on ice before use. The hepatic uptake was evaluated for the initial uptake rate by collecting aliquots at short time intervals (e.g. 20sec, 45sec and 90sec; or 30sec, 60sec and 120sec) up to 30min at 37°C in the presence or absence of 1 mM rifamycin SV. The passive diffusion was also assessed on ice with assumption that all the active uptake is abolished at 4°C. After 5 min preincubation at 37°C or on ice, the uptake was initiated by adding an equal volume of pre-warmed or pre-chilled KHB containing 2X test compound,

DMD Fast Forward. Published on August 5, 2020 as DOI: 10.1124/dmd.120.000064
This article has not been copyedited and formatted. The final version may differ from this version.

resulting in the final test compound concentration of 1 µM and cell concentration of 0.5 x 10^6 cells/mL. At designated time, an 80-µL aliquot of the reaction were removed and loaded onto a 0.4 ml centrifugation tube (Thermo Fisher Scientific) containing 100 µL of silicone-mineral oil layer (5:1 ratio, density of 1.015 g/mL) over 50 µL of 2M ammonium acetate to separate the hepatocytes from the reaction buffer. The top layer media samples and hepatocyte pellets were vortex-mixed with quenching solution (80% acetonitrile with 0.1% formic acid containing internal standard, 100 nM tolbutamide). After centrifugation at 4000 rpm for 20 min, the supernatants were analyzed by LC-MS/MS using API 5500 triple quadrupole mass spectrometer with Turbo Ion Spray source in MRM mode (AB Sciex, Foster City, CA) (supplemental method).

Rat PK study

The intravenous PK studies in rats were conducted at Syngene International Limited (Bangalore, India). Male Sprague-Dawley (SD) rats, 8-10 weeks old weighing between 250-350 g, were dosed either rosuvastatin, fluvastatin, cerivastatin or pravastatin (each prepared in 100% DMSO) at 1 mg per kg single dose, via i.v. bolus injected in femoral vein. The dosing volume was controlled at 0.5 mL/kg. Serial blood sampling was done via jugular vein at 0.083, 0.25, 0.5, 1, 2, 4, 6, 8 and 24 hours post-dose. Blood Samples collected in K2-EDTA tubes were placed on ice until centrifuged (at 4˚C, 10 minutes at 13000 rpm, within 30 minutes of collection) to separate plasma. Plasma samples were stored at -70˚C until LC-MS/MS analysis.

Data analysis

DMD Fast Forward. Published on August 5, 2020 as DOI: 10.1124/dmd.120.000064
This article has not been copyedited and formatted. The final version may differ from this version.

Approach 1: Determination of initial hepatic uptake CL ($PS_{u,inf}$) from in vitro hepatocyte uptake assay

The initial uptake rate was estimated from the slope obtained from the time course data within the initial linear phase, usually first three time points (20sec, 45sec and 90sec; or 30sec, 60sec and 120sec) using linear regression analysis. In the absence of BSA, the uptake CL (PS_{inf}) were calculated by dividing the initial uptake velocity by the total drug concentration measured in the incubation buffer. Assuming minimal binding in the aqueous buffer, PS_{inf} is equal to $PS_{u,inf}$. In the presence of BSA, the uptake CL ($PS_{u,inf}$) were determined by dividing the initial uptake velocity by the unbound drug concentrations in the incubation buffer containing 4% BSA.

$$PS_{u,inf} = \frac{PS_{inf}}{f_{u,KHB\ w\ 4\%\ BSA}}$$

$$PS_{u,inf} = PS_{u,act} + PS_{u,dif}$$

Approach 2: Determination of Kp_{uu} in rat hepatocytes

Determination of $Kp_{uu,ss}$ in rat hepatocytes based on steady-state uptake: The time-dependent uptake profiles for the transporter substrates were limited to 30 min to ensure good viability of hepatocytes. For most of the compounds, the uptake peaked or reached plateau at 5 or 15 min. Based on the assumptions that the active uptake and efflux in hepatocytes is completely ceased on ice and the fraction unbound in the cell at steady state is independent of temperature, the Kp_{uu} can be determined as Kp ratio of 37°C vs. 4°C at steady-state ($Kp_{uu,ss}$).

In the absence of BSA, at steady state, it is assumed to reach equilibrium between intracellular compartment and media, so $C_{u,cell}$ (4°C) = $C_{u,media}$ (4°C) and $f_{u,cell}$ (4°C) = $f_{u,cell}$ (37°C)

In the absence of BSA, it is assumed that $f_{u,media}$ =1

DMD Fast Forward. Published on August 5, 2020 as DOI: 10.1124/dmd.120.000064
This article has not been copyedited and formatted. The final version may differ from this version.

$$f_{u,cell,4oC} = \frac{C_{u,cell\ (4^oC)}}{C_{cell\ (4^oC)}} = \frac{C_{u,media\ (4^oC)}}{C_{cell\ (4^oC)}} = \frac{1}{Kp_{4^oC}}$$

$$Kp_{uu,ss} = \frac{C_{u,cell\ 37^oC}}{C_{u,media\ 37^oC}} = \frac{C_{cell\ 37^oC} \times f_{u,cell}}{C_{media\ 37^oC} \times f_{u,media}} = \frac{Kp_{37^oC}}{Kp_{4^oC}}$$

In the presence of BSA, $f_{u,media}$ is $f_{u,KHB\ w\ 4\%\ BSA}$

$$f_{u,cell,on\ ice} = \frac{C_{u,cell\ (4^oC)}}{C_{cell\ (4^oC)}} = \frac{C_{u,media\ (4^oC)}}{C_{cell\ (4^oC)}} = \frac{C_{media\ (4^oC)} \times f_{u,KHB\ w\ 4\%BSA}}{C_{cell\ (4^oC)}} = \frac{f_{u,KHB\ w\ 4\%BSA}}{Kp_{4^oC}}$$

$$Kp_{uu,ss} = \frac{C_{u,cell\ 37^oC}}{C_{u,media\ 37^oC}} = \frac{C_{cell\ 37^oC} \times f_{u,cell}}{C_{media\ 37^oC} \times f_{u,KHB\ w\ 4\%BSA}} = \frac{Kp_{37^oC}}{Kp_{4^oC}}$$

Where the Kp was determined by the ratio of total hepatocyte concentration and media concentration at 15 min.

When the hepatic uptake reaches steady-state in vitro, the unbound hepatocyte-to-medium concentration ratio (Kp_{uu}) can be also determined as equation below:

$$Kp_{uu,ss} = \frac{C_{u,cell,ss}}{C_{u,media,ss}} = \frac{C_{cell,ss} \times f_{u,cell}}{C_{media,ss} \times f_{u,media}} = Kp \times \frac{f_{u,cell}}{f_{u,media}}$$

In the absence of BSA, it is assumed that $f_{u,media}$ =1

$$Kp_{uu,ss} = Kp \times f_{u,cell}$$

In the presence of BSA,

$$Kp_{uu,ss} = Kp \times \frac{f_{u,cell}}{f_{u,KHB\ w\ 4\%\ BSA}}$$

Where the $f_{u,cell}$ and $f_{u,KHB\ w\ 4\%\ BSA}$ were experimentally determined in the binding assay.

DMD Fast Forward. Published on August 5, 2020 as DOI: 10.1124/dmd.120.000064
This article has not been copyedited and formatted. The final version may differ from this version.

Determination of $K_{puu,V0}$ in rat hepatocytes based on initial uptake rate: CL_{uptake} consists of active uptake ($PS_{inf,act}$) and passive diffusion ($PS_{inf,dif}$). PS_{inf} was determined by the initial hepatic uptake CL determined at 37°C; while the PS_{dif} was determined by the initial hepatic uptake CL determined at 37°C in the presence of uptake inhibitor, rifamycin-SV. Based on the extended clearance concept, assuming that the PS_{dif} for the cellular influx is equal to that for the efflux, $K_{p,uu}$ based on the initial uptake rate can be calculated using:

$$Kp_{uu,V0} = \frac{PS_{inf}}{PS_{dif}} = \frac{PS_{act} + PS_{dif}}{PS_{dif}}$$

In vitro to In Vivo Extrapolation (IVIVE) for Hepatic CL:

The intrinsic hepatocyte metabolic CL ($CL_{int,\ met}$ µL/min/10^6 cells) was determined in the absence of BSA in rat hepatocytes and the in vitro unbound hepatic uptake CL ($PS_{u,inf}$, µL/min/10^6 cells) were first scaled up to in vivo using the following physiologic scaling factor: 108 million cells/g liver and 36 g liver/Kg body weight (SimCYP).

According to the extended clearance concept (Sirianni and Pang 1997, Shitara et al. 2006, Kusuhara and Sugiyama 2009, Patilea-Vrana and Unadkat 2016), the hepatic intrinsic clearance ($CL_{int,\ all}$) is described by the following equation:

$$Cl_{int,all} = \left(PS_{inf,act} + PS_{inf,dif}\right) \times \frac{CL_{int,met+bile}}{PS_{eff,act} + PS_{eff,dif} + CL_{int,met+bile}}$$

Where $PS_{inf,act}$, $PS_{inf,dif}$, $PS_{eff,act}$, $PS_{eff,dif}$ and $CL_{int,\ met+bile}$ represents transporter mediated active uptake intrinsic CL, intrinsic passive diffusion influx CL, intrinsic transporter-mediated active efflux CL, intrinsic passive diffusion sinusoidal efflux CL, and the sum of intrinsic metabolic clearance ($CL_{int,\ met}$) and biliary excretion ($CL_{int,\ bile}$).

DMD Fast Forward. Published on August 5, 2020 as DOI: 10.1124/dmd.120.000064
This article has not been copyedited and formatted. The final version may differ from this version.

If $CL_{int,\ met+bile}$ is much higher than the total back flux ($PS_{eff,\ dif}$, and $PS_{eff,act}$), then $CL_{int,\ all}$ can be described as following:

$$Cl_{int,all} = PS_{inf,act} + PS_{inf,dif}$$

The equation can be rewritten as the following:

$$Cl_{int,all} = \left(CL_{int,met+bile}\right) \times \frac{PS_{inf,act} + PS_{inf,dif}}{PS_{eff,act} + PS_{eff,dif} + CL_{int,met+bile}}$$

Where ($PS_{inf,act}$ + $PS_{inf,dif}$)/($PS_{eff,act}$ + $PS_{eff,dif}$ + $CL_{int,\ met+bile}$) represents to the degree of hepatocellular unbound drug accumulation or the liver to plasma drug unbound concentration ratio (Kp_{uu}) at steady state. For the compounds which are actively taken up by hepatic uptake transporters and eliminated primarily by enzymatic metabolism, the equation is described as follows:

$$CL_{int,all} = CL_{int,met} \times Kp_{uu}$$

The predicted overall hepatic intrinsic clearance, by the above described methods, was used to predict systemic plasma clearance (CL_H) mediated by hepatic elimination using well-stirred model (Pang and Rowland 1977),

$$CL_H = Q_H \times \frac{CL_{int} \times f_{u,p}}{CL_{int} \times \frac{f_u}{R_{B/P}} + Q_H}$$

where CL_{int}, Q_H, $f_{u,p}$ and $R_{B/P}$ represent the predicted intrinsic hepatic CL, rat hepatic blood blow (77 mL/min/kg), unbound fraction in rat plasma and blood to plasma ratio, respectively.

DMD Fast Forward. Published on August 5, 2020 as DOI: 10.1124/dmd.120.000064
This article has not been copyedited and formatted. The final version may differ from this version.

The hepatic CL predicted by each IVIVE method was compared with the observed systemic CL. As the renal CL in rat for all the selected compounds are minimal (<10%), the total plasma clearance (CL_P) was used as surrogate of hepatic CL.

Statistical Analysis:

The prediction performance of each IVIVE approach used in the study was compared with observed hepatic CL in rat. The fold error, absolute average fold error (AAFE) and root mean squared logarithmic error (RMSE) were calculated as the following equations:

$$fold\ error\ = 10^{\left|Log_{10}\left(\frac{CL_{pred}}{CL_{observed}}\right)\right|}$$

$$AAFE\ = \ 10^{\left[\frac{1}{n}\Sigma\left|Log\left(\frac{CL_{pred}}{CL_{observed}}\right)\right|\right]}$$

$$RMSLE = \sqrt{\frac{1}{n}\sum\left(Log\ (CL_{pred}+1) - Log(CL_{observed}+1)\right)^2}$$

DMD Fast Forward. Published on August 5, 2020 as DOI: 10.1124/dmd.120.000064
This article has not been copyedited and formatted. The final version may differ from this version.

Results

Physicochemical Properties and In Vitro ADME data of Selected OATP Substrates. Twelve structurally diverse organic anion drugs covering a broad spectrum of physicochemical properties were systematically selected on the basis of varying permeability and lipophilicity. Compounds with high lipophilicity and high permeability include fluvastatin, cerivastatin, atorvastatin, bosentan, telmisartan, pitavastatin, nateglinide and glyburide; compounds with lower lipophilicity and low permeability include rosuvastatin, pravastatin and valsartan; compound with high lipophilicity and low permeability includes asunaprevir. The permeability, unbound fraction in all the matrices, including rat liver homogenate, KHB containing 4% BSA, rat plasma and rat hepatocytes incubation, and $CL_{int,\ met}$ in rat hepatocytes were determined and summarized in **Table 1** along with the physicochemical properties for each compound. The overall Log D at pH 7.4 spans from -2.7 to 4.0; and the permeability spans from 0.14 to 29 (10^{-6}cm/s). The unbound fractions in KHB with 4% BSA ($f_{u,\ KHB\ w\ 4\%\ BSA}$) were within 2-3 fold of the unbound fractions in rat plasma ($f_{u,p}$) for pravastatin, valsartan, fluvastatin, cerivastatin and atorvastatin. For the rest of compounds, the difference of $f_{u,\ KHB\ w\ 4\%\ BSA}$ value with $f_{u,p}$ value was greater than 3-fold. The $f_{u,p}$ values for almost all drugs except rosuvastatin and pravastatin were less than 0.05; and $f_{u,p}$ values for valsartan, pitavastatin, bosentan, glyburide and telmisartan were less than 0.01. For the drugs with highest lipophilicity, i.e., telmisartan and asunaprevir, the unbound fraction in rat liver homogenate for was less than 0.01, suggesting high non-specific binding for these two compounds.

Effect of Albumin on Hepatic Uptake CL in Rat Hepatocyte Suspension. The time-dependent uptake profile was determined in rat hepatocyte suspension in the absence and presence of 4% BSA (**Figure 1**). The uptake velocity at 4ºC of all the test compounds was

DMD Fast Forward. Published on August 5, 2020 as DOI: 10.1124/dmd.120.000064
This article has not been copyedited and formatted. The final version may differ from this version.

significantly lower than that at 37°C. In the presence of hepatic uptake transporter inhibitor, rifamycin-SV, the uptake at 37°C significantly decreased for all of the compounds confirming the involvement of active uptake transporters. However, only for the less permeable compounds, i.e., rosuvastatin, pravastatin and valsartan, the uptake at 37°C was reduced to the levels similar to 4°C. With addition of BSA, the dynamic range of active uptake (uptake at 37°C vs uptake at 37°C with inhibitor) improved, particularly for the two highly lipophilic drugs with high non-specific binding, asunaprevir (from less than 2-fold to 4-fold) and telmisartan (from 3-fold to 6-fold). In the absence of BSA, the uptake of all the drugs increased in a time-dependent manner except for telmisartan. The uptake of telmisartan reached a steady-state instantaneously due to its high binding characteristic, resulting in instant binding onto the cell surface. Therefore, the PS_{inf} at 37°C of telmisartan was not determined in the pure aqueous buffer system. In the presence of BSA, the uptake of all the drugs increased in a time-dependent manner. Initial hepatic uptake CL (PS_{inf}) was determined from the initial slopes of uptake measured in KHB and KHB containing 4% BSA, respectively (**Table 2**). In the presence of BSA, the hepatic uptake CL for unbound drug ($PS_{u,inf}$) was calculated by dividing PS_{inf} by $f_{u,\ KHB\ w\ 4\%BSA}$ value. In the regular KHB, unbound fraction in the media was assumed to be unity, therefore, the $PS_{u,inf}$ was equal to PS_{inf}. In the absence of BSA, $PS_{u,inf}$ ranged from 8.9 (pravastatin) to 2210 (asunaprevir) µL/min/10^6 cells; and in the presence of BSA, $PS_{u,inf}$ ranged from 10.3 (pravastatin) to 2668 (asunaprevir) µL/min/10^6 cells. In the presence of BSA, the PS_{inf} values for almost all drugs except pravastatin decreased compared to PS_{inf} values determined in the absence of BSA. However, the $PS_{u,inf}$ with BSA overall increased, but to different extent, when compared to $PS_{u,inf}$ without BSA: for rosuvastatin, cerivastatin, pravastatin, atorvastatin, bosentan, asunaprevir, and nateglinide, this increase was less than 2- fold; for fluvastatin, pitavastatin and glyburide, the

DMD Fast Forward. Published on August 5, 2020 as DOI: 10.1124/dmd.120.000064
This article has not been copyedited and formatted. The final version may differ from this version.

increase was within 2-3 fold; for valsartan and telmisartan, the increase was greater than 10- fold. These results demonstrated that drugs with high plasma protein binding vary in the level of "albumin-mediated" hepatic uptake. Additionally, based on these data we were unable to identify any specific trends related to permeability or lipophilicity of the compounds which would dictate the enhanced hepatic uptake in the presence of BSA.

Effect of Albumin on Kp_{uu} Determination in Rat Hepatocytes. The Kp_{uu} values of the twelve OATP substrates were determined in the absence and presence of BSA using temperature method, homogenization method and initial rate method as described in the Materials and Methods section. The data are summarized in **Table 3**. Based on the time profiles, the uptake of most drugs peaked at 15min, then either plateaued or started to decline. For both temperature method and homogenization method, the $Kp_{uu,\,ss}$ were determined at 15min for all the compounds, except valsartan determined at 30min of uptake. By using the temperature method, the difference of $Kp_{uu,ss}$ values determined in the absence or presence of BSA were mostly within 2-3 fold. In contrast, using homogenization method in general resulted in an increase in the $Kp_{uu,ss}$ values, except for rosuvastatin, pravastatin and bosentan. The increase was substantial (greater than 7-fold) for valsartan, telmisartan and glyburide; for the rest of compounds, the increase was within 2- fold. PS_{inf} and $PS_{inf,dif}$ were determined from the initial slope of uptake at 37^{o}C and 37^{o}C with inhibitor, respectively. The $Kp_{uu,V0}$ calculated based on ratio of PS_{inf} and $PS_{inf,dif}$ determined in the absence and presence of BSA are summarized in **Table 3**. The impact of BSA on the $Kp_{uu,V0}$ does not have a clear trend due to the relatively large inter-experimental variability. $Kp_{uu,V0}$ for telmisartan in the absence of BSA cannot be determined due to the high non-specific binding.

In vitro to in vivo Extrapolation of Hepatic CL. The hepatic CL predicted by three IVIVE approaches using 1) $CL_{int,\,met}$ alone; 2) corrected $CL_{int,\,met}$ by Kp_{uu}; 3) $PS_{u,inf}$, were compared with

DMD Fast Forward. Published on August 5, 2020 as DOI: 10.1124/dmd.120.000064
This article has not been copyedited and formatted. The final version may differ from this version.

in vivo observed hepatic CL in rat (**Figure 2**). First, when applying the traditional IVIVE approach by scaling directly from intrinsic metabolic CL alone, the hepatic CL was significantly underestimated for majority of the compounds and the AAFE and RMSLE were 8.99 and 0.83 respectively (**Table 5**). Only one compound (atorvastatin) fell within 3-fold error, and 6 out of 12 compounds showed greater than 10-fold underestimation of the hepatic CL (**Figure 2A and Table 4**).

Based on the extended clearance concept, in the scenario when hepatic uptake is the rate-determining step for hepatic CL, the intrinsic hepatic CL could be well accounted for by the in vitro hepatic uptake CL, regardless of the involvement of hepatic metabolism. $PS_{u,inf}$ determined in the hepatic uptake assay was used to predict the systemic hepatic CL (**Figure 2B, Table 2**). In the absence of BSA, 5 out of 12 compounds fell within the 3-fold error; 9 out of 12 compounds fell within 5-fold error; two compounds (valsartan and nateglinide) showed great than 10-fold underestimation; this approach was not applicable for telmisartan as $PS_{u,inf}$ could not be determined. In the presence of BSA, the predictability of $PS_{u,inf}$ was improved as demonstrated by AAFE and RMSLE (3.48 and 0.58 without BSA vs 2.23 and 0.40 with BSA) (**Table 5**); 8 out of 12 compounds fell within the 3-fold error and 11 out of 12 compounds fell within 5-fold error; only one compound (nateglinide) was underestimated greater than 5 fold.

According to the extended clearance concept, correcting $CL_{int,\ met}$ determined in rat hepatocytes by multiplying Kp_{uu} substantially improved the prediction of hepatic CL for all of the 12 compounds (**Table 4**). When using the $Kp_{uu,ss}$ determined by temperature method in the absence of BSA, the prediction of 10 out 12 compounds fell within the 3-fold error, and only one compound (telmisartan) showed greater than 5-fold underestimation of the hepatic CL (**Figure 2C**). In the presence of BSA, the prediction performance was similar with the condition without

DMD Fast Forward. Published on August 5, 2020 as DOI: 10.1124/dmd.120.000064
This article has not been copyedited and formatted. The final version may differ from this version.

BSA, as demonstrated by AAFE and RMSLE (1.95 and 0.32 without BSA vs 2.11 and 0.37 with BSA) (**Table 5**). When using the $Kp_{uu,ss}$ determined by homogenization method, in the absence of BSA, 6 out of 12 compounds fell within the 3-fold error and four compounds (valsartan, telmisartan, asunaprevir and nateglinide) showed greater than 5-10 fold underestimation (**Figure 2D**). In contrast, the prediction performance was significantly improved by applying BSA when using the homogenization method, as demonstrated by AAFE and RMSLE (3.72 and 0.58 without BSA vs 2.0 and 0.35 with BSA) (**Table 5**). When using the $Kp_{uu,v0}$ determined by the ratio of PS_{inf} and $PS_{inf,dif}$, 9 out of 12 compounds fell within the 3-fold error regardless of the presence of BSA (**Figure 2E**). Although, the prediction performance of the $Kp_{uu,v0}$ approach looked reasonable, however, due to the large inter-experimental variation of $Kp_{uu,v0}$ determination, this method is not practically recommended.

DMD Fast Forward. Published on August 5, 2020 as DOI: 10.1124/dmd.120.000064
This article has not been copyedited and formatted. The final version may differ from this version.

Discussion

Accurate human PK prediction is pivotal at early stages of drug discovery to manage human dose projection, estimate efficacy and safety margins in an integrated manner. With the success in reducing CYP-mediated CL, the current chemical matter of interest has become more metabolically stable and transporter-mediated CL mechanisms have become predominant drivers of clearance (Shitara et al. 2006, International Transporter et al. 2010, Jones et al. 2012). A practical approach to accurately predict transporter mediated CL is urgently needed in the field to guide the prioritization of the new molecular entities with suitable PK properties for clinical development. Gaining the confidence in IVIVE strategies in preclinical species is an essential step towards improved human PK prediction. Rat is the most commonly used preclinical species for evaluating PK of drug candidates in early drug discovery. Therefore, this study focused on establishing a robust in vitro uptake assay in rat hepatocytes and evaluate variety of IVIVE approaches to provide a practical solution for predicting hepatic uptake transporter-mediated clearance in rat.

It has also been demonstrated that the intrinsic hepatic uptake CL determined in human hepatocytes suspension was far more predictive of in vivo clearance of statins than extrapolating from intrinsic metabolic clearance (Watanabe et al. 2010, Watanabe et al. 2011). However, this approach is restricted to highly lipophilic compounds, due to the inability to detect active transport activity due to the high background caused by the high permeability, and underestimation of the intrinsic hepatic uptake clearance due to the non-specific binding (Kim et al. 2019, Koyanagi et al. 2019). Several studies have reported that addition of albumin can improve the IVIVE for hepatic uptake transporter substrates (Kim et al. 2019, Koyanagi et al. 2019, Riccardi et al. 2019). Therefore, in the current study, we investigated the impact of BSA at

DMD Fast Forward. Published on August 5, 2020 as DOI: 10.1124/dmd.120.000064
This article has not been copyedited and formatted. The final version may differ from this version.

physiologically relevant concentrations on the predictability of the hepatic uptake parameters determined in suspended rat hepatocytes using various approaches.

Compared to the traditional IVIVE approach from $CL_{int, met}$ alone, both advanced approaches ($PS_{u,inf}$ and the corrected $CL_{int, met}$ by Kp_{uu}) substantially improved the prediction of hepatic CL for all twelve selected drugs. Among all the conditions evaluated in this study, $PS_{u,inf}$ generated in the presence of 4% BSA and $CL_{int, met}$ multiplied by $Kp_{uu,ss}$ generated using homogenization method in the presence of BSA and temperature method showed the most robust correlation with systemic hepatic CL. Some compounds are equally well predicted by all the approaches tested, regardless of addition of BSA, for examples, rosuvastatin, fluvastatin, cerivastatin, atorvastatin, and bosentan; the compounds which are sensitive to the IVIVE approaches and the presence of BSA include pravastatin, valsartan, telmisartan, asunaprevir, pitavastatin, nateglinide and glyburide.

For 8 out of 12 compounds, $PS_{u,inf}$ value determined in the presence of BSA is similar to that in the absence of BSA; two compounds (fluvastatin and glyburide) showed about 3-fold increase of $PS_{u,inf}$ value in the presence of BSA; two compounds (valsartan and telmisartan) demonstrated greater than 10-fold increase in $PS_{u,inf}$ value in the presence of BSA. In contrast, the impact of albumin on the $PS_{u,inf}$ observed in human hepatocytes is more significant (unpublished data from our laboratory and (Kim et al. 2019). The increase of unbound intrinsic hepatic uptake in the presence of BSA can be attributed to albumin-mediated hepatic uptake. The “facilitated-dissociation” model has been proposed recently to explain the phenomena where interaction of the albumin-drug complex with the cell surface enhances dissociation of the complex to present more unbound drug molecules to be transported (Miyauchi et al. 2018, Kim et al. 2019). Another group proposed transporter-induced protein binding shift model, where high affinity binding to

DMD Fast Forward. Published on August 5, 2020 as DOI: 10.1124/dmd.120.000064
This article has not been copyedited and formatted. The final version may differ from this version.

transporters may strip ligands off of the plasma protein before they dissociate (Bowman et al. 2019). Based on these theories, the compounds with low binding to albumin should show less change in the $PS_{u,inf}$ in the presence of BSA, while addition of BSA should demonstrate higher impact on the compounds with high binding to albumin. However, our data indicated the impact of albumin on the $PS_{u,inf}$ was not always shown for the compounds with high protein binding ($f_{u,p}$ < 0.01), i.e., bosentan and pitavastatin. Our finding suggested that the "albumin-mediated" hepatic uptake phenomenon could vary among compounds or between species, which may be attributed to interspecies difference in albumin binding, and expression or function of hepatic uptake transporters between human and rat. The relationship of albumin-mediated transport with variety of molecule properties requires further investigations, i.e., in-silico prediction (Liu et al. 2016). It is important to note that there may be difference in protein binding between rat plasma protein and BSA as well. The compound avidly bound to albumin may have strong non-specific binding to cell surface or assay device due to the high lipophilicity. In the aqueous buffer, the loss of compounds in the nominal concentration could be another reason of underestimation in the in vitro assay. Therefore, it is important to calculate the $PS_{u,inf}$ using experimentally measured media concentration.

Several in vitro methods have been developed and utilized to estimate the value of Kp_{uu}. The temperature method refers to $Kp_{uu,ss}$ estimated in hepatocytes using $f_{u,\ liver}$ determined by 1/Kp at 4ºC based upon the assumptions that active transport is completely abolished on ice and tissue binding is not temperature-dependent (Shitara et al. 2013, Riede et al. 2017, Yoshikado et al. 2017). Ryu, et al. have demonstrated that the drug binding properties are not influenced by assay temperature (Ryu et al. 2018). Our study showed $Kp_{uu,ss}$ estimated using temperature method was not impacted by addition of BSA, and $CL_{int,met}$ corrected by this $Kp_{uu,ss}$ demonstrated the most

DMD Fast Forward. Published on August 5, 2020 as DOI: 10.1124/dmd.120.000064
This article has not been copyedited and formatted. The final version may differ from this version.

robust correlation with in vivo observed rat CL, which provide experimental evidence of vitality of these assumptions.

The homogenization method refers to $Kp_{uu,ss}$ determined using experimentally measured $f_{u,\ liver}$ in liver homogenate. The fundamental assumption of this method is that drug binding to the intracellular compartment is not affected by the homogenization process. For the least bound drug, i.e., pravastatin and the drug with high molecular weight, i.e., asunaprevir, the $Kp_{uu,ss}$ generated using this method was significantly lower compared to other methods. This phenomenon may be associated with the native caveat of the method for measuring the f_u in tissue/cell homogenate (Riede et al. 2017). Mechanical homogenization which not only disrupt the plasma membrane but also break subcellular organelles, results in increased number of intracellular binding sites to the drugs (de Araujo et al. 2015, Keemink et al. 2015). Hence, $f_{u,\ liver}$ for the compounds with less lipophilicity or higher molecular weight can be underestimated. In addition, for the compounds with high binding to plasma, i.e., valsartan, telmisartan, and glyburide, $Kp_{uu,ss}$ estimated using this method was significantly enhanced by supplementing the uptake assay with 4% BSA, subsequently leading to improved hepatic CL prediction, which can be contributed by two factors, 1) albumin mediated hepatic uptake and/or 2) reduced non-specific binding of test compounds to the cell surface or assay device.

The initial rate method refers to $Kp_{uu,v0}$ determined from the initial active uptake and passive diffusion (Yabe et al. 2011). Comparatively, the $Kp_{uu,\ ss}$ method has a practical advantage over the method to obtain the $Kp_{uu,\ V0}$ value, as the experimental variability is much less for measuring $Kp_{uu,ss}$ than for $Kp_{uu,\ V0}$, at least in our hands. The uptake data at longer time (15min or 30min, ~ steady state) are enough for $Kp_{uu,ss}$ estimation, whereas initial uptake rates obtained within seconds are required for $Kp_{uu,\ V0}$ determination. Thus complexity in the assay procedure such a

DMD Fast Forward. Published on August 5, 2020 as DOI: 10.1124/dmd.120.000064
This article has not been copyedited and formatted. The final version may differ from this version.

rapid sampling at quick intervals could be a practical limitation of the latter approach. As $Kp_{uu,v0}$ is determined by PS_{inf} and PS_{dif}, the impact of BSA on the $Kp_{uu,\ v0}$ should be aligned with the effect of BSA on PS_{inf}, if PS_{dif} is not influenced by addition of BSA. The large assay variation mainly attributed to PS_{dif} determined at $37^{o}C$ with hepatic uptake inhibitor. The phenomena of albumin-mediated hepatic uptake has been only investigated at the level of total influx. Therefore, the impact of albumin on active uptake vs. passive diffusion, and on other uptake (e.g. OATs) and efflux (e.g. MRPs) transporters would require further investigation.

In conclusion, this study has demonstrated that the hepatic CL mediated by OATP transporter can be predicted reasonably well based upon extended clearance concept regardless of the involvement of metabolism and lipophilicity of the test compounds. Taking into account the assumptions and practical limitation of all the investigated methods, both intrinsic hepatic uptake CL determined in rat hepatocyte suspension in the presence of 4% BSA, and adjusted $CL_{int,met}$ by hepatocyte to media unbound concentration ratio determined in rat hepatocytes suspension at steady state provided robust correlation with the observed in vivo rat hepatic CL without any empirical scaling factor. In light of these findings, this study provided a practical strategy for improved predictions of transporter-mediated hepatic CL to support the optimization of new molecular entities in the early stage of drug discovery. The establishment of IVIVC in preclinical stage will build our confidence in human PK prediction as a necessary step toward the first-in-human study.

DMD Fast Forward. Published on August 5, 2020 as DOI: 10.1124/dmd.120.000064
This article has not been copyedited and formatted. The final version may differ from this version.

Acknowledgements

Authors would like to acknowledge Q^2 Solutions for permeability measurements and Syngene International Limited for rat in vivo PK studies. Authors would also like to thank Dan Rock, Jan Wahlstrom, and Dean Hickman for their support of this work.

DMD Fast Forward. Published on August 5, 2020 as DOI: 10.1124/dmd.120.000064
This article has not been copyedited and formatted. The final version may differ from this version.

Authorship Contributions

Participated in research design: Na Li, Akshay Badrinarayanan, Anshul Gupta

Conducted experiments: Na Li, Akshay Badrinarayanan, Xingwen Li, John Roberts, Mike Hayashi, Manpreet Virk

Performed data analysis: Na Li, Akshay Badrinarayanan, Anshul Gupta

Wrote or contributed to the writing of the manuscript: Na Li, Anshul Gupta, Akshay Badrinarayanan, John Roberts and Mike Hayashi

DMD Fast Forward. Published on August 5, 2020 as DOI: 10.1124/dmd.120.000064
This article has not been copyedited and formatted. The final version may differ from this version.

References

Bowman, C. M., H. Okochi and L. Z. Benet (2019). "The Presence of a Transporter-Induced Protein Binding Shift: A New Explanation for Protein-Facilitated Uptake and Improvement for In Vitro-In Vivo Extrapolation." Drug Metab Dispos **47**(4): 358-363.

de Araujo, M. E., G. Lamberti and L. A. Huber (2015). "Homogenization of Mammalian Cells." Cold Spring Harb Protoc **2015**(11): 1009-1012.

Di, L., C. Keefer, D. O. Scott, T. J. Strelevitz, G. Chang, Y. A. Bi, Y. Lai, J. Duckworth, K. Fenner, M. D. Troutman and R. S. Obach (2012). "Mechanistic insights from comparing intrinsic clearance values between human liver microsomes and hepatocytes to guide drug design." Eur J Med Chem **57**: 441-448.

Hallifax, D., J. A. Foster and J. B. Houston (2010). "Prediction of human metabolic clearance from in vitro systems: retrospective analysis and prospective view." Pharm Res **27**(10): 2150-2161.

Hirano, M., K. Maeda, Y. Shitara and Y. Sugiyama (2004). "Contribution of OATP2 (OATP1B1) and OATP8 (OATP1B3) to the hepatic uptake of pitavastatin in humans." J Pharmacol Exp Ther **311**(1): 139-146.

International Transporter, C., K. M. Giacomini, S. M. Huang, D. J. Tweedie, L. Z. Benet, K. L. Brouwer, X. Chu, A. Dahlin, R. Evers, V. Fischer, K. M. Hillgren, K. A. Hoffmaster, T. Ishikawa, D. Keppler, R. B. Kim, C. A. Lee, M. Niemi, J. W. Polli, Y. Sugiyama, P. W. Swaan, J. A. Ware, S. H. Wright, S. W. Yee, M. J. Zamek-Gliszczynski and L. Zhang (2010). "Membrane transporters in drug development." Nat Rev Drug Discov **9**(3): 215-236.

Izumi, S., Y. Nozaki, T. Komori, O. Takenaka, K. Maeda, H. Kusuhara and Y. Sugiyama (2017). "Comparison of the Predictability of Human Hepatic Clearance for Organic Anion Transporting Polypeptide Substrate Drugs Between Different In Vitro-In Vivo Extrapolation Approaches." J Pharm Sci **106**(9): 2678-2687.

Jones, H. M., H. A. Barton, Y. Lai, Y. A. Bi, E. Kimoto, S. Kempshall, S. C. Tate, A. El-Kattan, J. B. Houston, A. Galetin and K. S. Fenner (2012). "Mechanistic pharmacokinetic modeling for the prediction of transporter-mediated disposition in humans from sandwich culture human hepatocyte data." Drug Metab Dispos **40**(5): 1007-1017.

Kalvass, J. C., T. S. Maurer and G. M. Pollack (2007). "Use of plasma and brain unbound fractions to assess the extent of brain distribution of 34 drugs: comparison of unbound concentration ratios to in vivo p-glycoprotein efflux ratios." Drug Metab Dispos **35**(4): 660-666.

Keemink, J., P. Augustijns and P. Annaert (2015). "Unbound ritonavir concentrations in rat and human hepatocytes." J Pharm Sci **104**(7): 2378-2387.

Kilford, P. J., R. Stringer, B. Sohal, J. B. Houston and A. Galetin (2009). "Prediction of drug clearance by glucuronidation from in vitro data: use of combined cytochrome P450 and UDP-glucuronosyltransferase cofactors in alamethicin-activated human liver microsomes." Drug Metab Dispos **37**(1): 82-89.

Kim, S. J., K. R. Lee, S. Miyauchi and Y. Sugiyama (2019). "Extrapolation of In Vivo Hepatic Clearance from In Vitro Uptake Clearance by Suspended Human Hepatocytes for Anionic Drugs with High Binding to Human Albumin: Improvement of In Vitro-to-In Vivo Extrapolation by Considering the "Albumin-Mediated" Hepatic Uptake Mechanism on the Basis of the "Facilitated-Dissociation Model"." Drug Metab Dispos **47**(2): 94-103.

Koyanagi, T., K. Yano, S. Kim, N. Murayama, H. Yamazaki and I. Tamai (2019). "In vivo hepatic clearance of lipophilic drugs predicted by in vitro uptake data into cryopreserved hepatocytes suspended in sera of rats, guinea pigs, monkeys and humans." Xenobiotica **49**(8): 887-894.

Kusuhara, H. and Y. Sugiyama (2009). "In vitro-in vivo extrapolation of transporter-mediated clearance in the liver and kidney." Drug Metab Pharmacokinet **24**(1): 37-52.

Li, R., H. A. Barton and M. V. Varma (2014). "Prediction of pharmacokinetics and drug-drug interactions when hepatic transporters are involved." Clin Pharmacokinet **53**(8): 659-678.

Liu, H. C., A. Goldenberg, Y. Chen, C. Lun, W. Wu, K. T. Bush, N. Balac, P. Rodriguez, R. Abagyan and S. K. Nigam (2016). "Molecular Properties of Drugs Interacting with SLC22 Transporters OAT1, OAT3, OCT1, and OCT2: A Machine-Learning Approach." J Pharmacol Exp Ther **359**(1): 215-229.
Miyauchi, S., M. Masuda, S. J. Kim, Y. Tanaka, K. R. Lee, S. Iwakado, M. Nemoto, S. Sasaki, K. Shimono, Y. Tanaka and Y. Sugiyama (2018). "The Phenomenon of Albumin-Mediated Hepatic Uptake of Organic Anion Transport Polypeptide Substrates: Prediction of the In Vivo Uptake Clearance from the In Vitro Uptake by Isolated Hepatocytes Using a Facilitated-Dissociation Model." Drug Metab Dispos **46**(3): 259-267.
Mosure, K. W., J. O. Knipe, M. Browning, V. Arora, Y. Z. Shu, T. Phillip, F. McPhee, P. Scola, A. Balakrishnan, M. G. Soars, K. Santone and M. Sinz (2015). "Preclinical Pharmacokinetics and In Vitro Metabolism of Asunaprevir (BMS-650032), a Potent Hepatitis C Virus NS3 Protease Inhibitor." J Pharm Sci **104**(9): 2813-2823.
Nakai, D., K. Kumamoto, C. Sakikawa, T. Kosaka and T. Tokui (2004). "Evaluation of the protein binding ratio of drugs by a micro-scale ultracentrifugation method." J Pharm Sci **93**(4): 847-854.
Pang, K. S. and M. Rowland (1977). "Hepatic clearance of drugs. I. Theoretical considerations of a "well-stirred" model and a "parallel tube" model. Influence of hepatic blood flow, plasma and blood cell binding, and the hepatocellular enzymatic activity on hepatic drug clearance." J Pharmacokinet Biopharm **5**(6): 625-653.
Patilea-Vrana, G. and J. D. Unadkat (2016). "Transport vs. Metabolism: What Determines the Pharmacokinetics and Pharmacodynamics of Drugs? Insights From the Extended Clearance Model." Clin Pharmacol Ther **100**(5): 413-418.
Rabbani, G. and S. N. Ahn (2019). "Structure, enzymatic activities, glycation and therapeutic potential of human serum albumin: A natural cargo." Int J Biol Macromol **123**: 979-990.
Riccardi, K. A., D. A. Tess, J. Lin, R. Patel, S. Ryu, K. Atkinson, L. Di and R. Li (2019). "A Novel Unified Approach to Predict Human Hepatic Clearance for Both Enzyme- and Transporter-Mediated Mechanisms Using Suspended Human Hepatocytes." Drug Metab Dispos **47**(5): 484-492.
Riede, J., G. Camenisch, J. Huwyler and B. Poller (2017). "Current In Vitro Methods to Determine Hepatic Kpuu: A Comparison of Their Usefulness and Limitations." J Pharm Sci **106**(9): 2805-2814.
Ryu, S., J. J. Novak, R. Patel, P. Yates and L. Di (2018). "The impact of low temperature on fraction unbound for plasma and tissue." Biopharm Drug Dispos **39**(9): 437-442.
Shitara, Y., T. Horie and Y. Sugiyama (2006). "Transporters as a determinant of drug clearance and tissue distribution." Eur J Pharm Sci **27**(5): 425-446.
Shitara, Y., K. Maeda, K. Ikejiri, K. Yoshida, T. Horie and Y. Sugiyama (2013). "Clinical significance of organic anion transporting polypeptides (OATPs) in drug disposition: their roles in hepatic clearance and intestinal absorption." Biopharm Drug Dispos **34**(1): 45-78.
Sirianni, G. L. and K. S. Pang (1997). "Organ clearance concepts: new perspectives on old principles." J Pharmacokinet Biopharm **25**(4): 449-470.
Tamura, M., S. Shiba, N. Kudo and Y. Kawashima (2010). "Pharmacokinetics of nateglinide enantiomers and their metabolites in Goto-Kakizaki rats, a model for type 2 diabetes mellitus." Chirality **22**(1): 92-98.
Tessari, P. (2003). "Protein metabolism in liver cirrhosis: from albumin to muscle myofibrils." Curr Opin Clin Nutr Metab Care **6**(1): 79-85.
Treiber, A., R. Schneiter, S. Delahaye and M. Clozel (2004). "Inhibition of organic anion transporting polypeptide-mediated hepatic uptake is the major determinant in the pharmacokinetic interaction between bosentan and cyclosporin A in the rat." J Pharmacol Exp Ther **308**(3): 1121-1129.
Tsao, S. C., Y. Sugiyama, Y. Sawada, T. Iga and M. Hanano (1988). "Kinetic analysis of albumin-mediated uptake of warfarin by perfused rat liver." J Pharmacokinet Biopharm **16**(2): 165-181.

Tsao, S. C., Y. Sugiyama, K. Shinmura, Y. Sawada, S. Nagase, T. Iga and M. Hanano (1988). "Protein-mediated hepatic uptake of rose bengal in analbuminemic mutant rats (NAR). Albumin is not indispensable to the protein-mediated transport of rose bengal." Drug Metab Dispos **16**(3): 482-489.
Watanabe, T., H. Kusuhara, K. Maeda, H. Kanamaru, Y. Saito, Z. Hu and Y. Sugiyama (2010). "Investigation of the rate-determining process in the hepatic elimination of HMG-CoA reductase inhibitors in rats and humans." Drug Metab Dispos **38**(2): 215-222.
Watanabe, T., H. Kusuhara, K. Maeda, Y. Shitara and Y. Sugiyama (2009). "Physiologically based pharmacokinetic modeling to predict transporter-mediated clearance and distribution of pravastatin in humans." J Pharmacol Exp Ther **328**(2): 652-662.
Watanabe, T., H. Kusuhara, T. Watanabe, Y. Debori, K. Maeda, T. Kondo, H. Nakayama, S. Horita, B. W. Ogilvie, A. Parkinson, Z. Hu and Y. Sugiyama (2011). "Prediction of the overall renal tubular secretion and hepatic clearance of anionic drugs and a renal drug-drug interaction involving organic anion transporter 3 in humans by in vitro uptake experiments." Drug Metab Dispos **39**(6): 1031-1038.
Wolfgang Wienen, M. E., 2Jacobus C. A. van Meel,, U. B. Joachim Stangier, Thomas Ebner, Jochen Schmid,, K. M. Horst Lehmann, 4Joan Kempthorne-Rawson, and a. N. H. H. 3Volker Gladigau (2000). "A Review on Telmisartan: A Novel, Long-Acting Angiotensin II-Receptor Antagonist." Cardiovascular Drug Reviews **18**(2): 127-154.
Yabe, Y., A. Galetin and J. B. Houston (2011). "Kinetic characterization of rat hepatic uptake of 16 actively transported drugs." Drug Metab Dispos **39**(10): 1808-1814.
Yamashiro, W., K. Maeda, M. Hirouchi, Y. Adachi, Z. Hu and Y. Sugiyama (2006). "Involvement of transporters in the hepatic uptake and biliary excretion of valsartan, a selective antagonist of the angiotensin II AT1-receptor, in humans." Drug Metab Dispos **34**(7): 1247-1254.
Yoshikado, T., K. Toshimoto, T. Nakada, K. Ikejiri, H. Kusuhara, K. Maeda and Y. Sugiyama (2017). "Comparison of Methods for Estimating Unbound Intracellular-to-Medium Concentration Ratios in Rat and Human Hepatocytes Using Statins." Drug Metab Dispos **45**(7): 779-789.
Zhou, X., L. R. Rougee, D. W. Bedwell, J. W. Cramer, M. A. Mohutsky, N. A. Calvert, R. D. Moulton, K. C. Cassidy, N. P. Yumibe, L. A. Adams and K. J. Ruterbories (2016). "Difference in the Pharmacokinetics and Hepatic Metabolism of Antidiabetic Drugs in Zucker Diabetic Fatty and Sprague-Dawley Rats." Drug Metab Dispos **44**(8): 1184-1192.

Footnotes

No funding is involved for this work.

DMD Fast Forward. Published on August 5, 2020 as DOI: 10.1124/dmd.120.000064
This article has not been copyedited and formatted. The final version may differ from this version.

Figure Legends

Figure 1. Time-dependent uptake of the 12 OATP substratesin cryopreserved rat hepatocyte suspension. Uptake of rosuvastatin (A), fluvastatin (B), cerivastatin (C), pravastatin (D), atorvastatin (E), pitavastatin (F), bosentan (G), glyburide (H), nateglinide (I), valsartan (J), asunaprevir (K) and telmisartan (L) at 1 μM was determined in the regular KHB (left column) or KHB containing 4% BSA (right column) for (20sec -30min) at 37^{o}C (closed circle), 37^{o}C in the presence of 1mM rifamycin-SV (open circle), or 4^{o}C (closed triangle). The uptake velocity (V_0) was calculated by dividing the amount of compound measured in rat hepatocytes at each time point by the total compound concentration in the reaction buffer in the absence or presence of 4% BSA. Data represents duplicate measurement at each time points.

Figure 2. Correlation of the predicted hepatic CL using different IVIVE approaches with the observed in vivo hepatic CL in rat. Predicted hepatic CL based on intrinsic metabolic CL determined in rat hepatocytes (A). Predicted hepatic CL based on initial hepatic uptake CL determined in rat hepatocytes suspension (B). The open diamond symbol represents the unbound initial uptake CL ($PS_{u,inf}$) determined in KHB containing 4% BSA; the blue circle represents the initial uptake CL ($PS_{u,inf}$) determined in KHB with no BSA. Predicted hepatic CL based upon the extended clearance concept, corrected intrinsic metabolic CL by Kp_{uu} determined using temperature method (C), homogenization method (D) and initial rate method (E). The open diamond symbol represents the Kp_{uu} determined in KHB containing 4% BSA; the blue circle represents the Kp_{uu} determined in the absence of 4% BSA.

Table 1. Physicochemical properties, unbound fraction in variety of matrices, intrinsic metabolic clearance in rat hepatocytes of the selected 12 compounds

	Physico-Chemical Properties				Ubound Fraction in Matrices				Intrinsic Metabolic CL
	M.W.	**Log $D_{7.4}$[a]**	**pKa[a]**	**P_{app} (10^{-6} cm/s)**	$f_{u,\ liver\ tissue}$	$f_{u,\ KHB\ w\ 4\%BSA}$	$f_{u,\ p}$	$f_{u,\ hep}$	**Rat Hepatocyte $CL_{int,met}$ (µL/min/10^6 Cells)**
Rosuvastatin	481.5	-2.7	4.3	1.8	0.15	0.21	0.059	0.7	19.8
Pravastatin	424.5	-0.8	4.3	0.62	0.29	0.69	0.63	0.8	NA
Valsartan	435.5	-0.6	3.7, 4.2	0.14	0.048[b]	0.006[c]	0.0029	0.7	20.4
Pitavastatin	421.5	0.4	4.2, 5.2	13	0.019	0.057	0.0065	0.5	46.2
Fluvastatin	411.5	0.5	4.3	19	0.015	0.037	0.015	0.5	38.8
Cerivastatin	459.6	0.6	4.2, 5.6	28	0.019	0.04	0.029	0.5	47.9
Nateglinide	317.4	0.6	3.6	6.2	0.037	0.063	0.015	0.7	43.5
Atorvastatin	558.6	1.3	4.3	5.5	0.018	0.066	0.036	0.6	90.8
Bosentan	551.6	1.5	4.0	16	0.025	0.057	0.0089	0.6	39.4
Glyburide	494.0	1.9	5.2	22	0.011	0.014	0.002	0.6	54.5
Asunaprevir	748.3	2.3	3.9, 5.6	1.7	0.00073	0.059	0.013	0.3	36.2
Telmisartan	514.6	4.0	3.5, 3.9, 5.0	29	0.0038	0.031	0.0061	0.45	23.3

NA, not available

[a] Predicted by Amgen in-silico model

[b] Data is referenced from (Li et al. 2014)

[c] Data is referenced from (Riccardi et al. 2019)

Table 2. Unbound Initial Hepatic Uptake Clearance Determined in the Presence and Absence of 4% BSA and Predicted Rat Hepatic Clearance

	Initial Hepatic Uptake Rate		Predicted Hepatic CL				Observed CL
	no BSA	w 4% BSA	no BSA		w 4% BSA		
Compound	$PS_{u,inf}$ (μL/min/10^6)	$PS_{u,inf}$ (μL/min/10^6)	CL_{int} (ml/min/kg)	Pred rat CL (ml/min/Kg)	CL_{int} (ml/min/kg)	Pred rat CL (ml/min/Kg)	Rat CL (mL/min/Kg)
Rosuvastatin	120 (126, 114)	221 ± 13.8	467	17.2	858	24.2	56.7
Pravastatin	8.87 (13.0, 4.73)	10.3 (7.49, 13.2)	34.5	14.8	40.2	16.4	59.7
Valsartan	34.0 ± 10.5	560 (404, 716)	132	0.4	2177	5.6	17.8[a]
Pitavastatin	249 (261, 236)	470 ± 212	966	5.5	1827	9.4	28[b]
Fluvastatin	277 (310, 244)	903 (710, 1095)	1077	12.0	3509	24.6	20.0
Cerivastatin	527 ± 110	798 (595, 1001)	2048	26.0	3103	30.5	24.7
Nateglinide	88.8 (82.4, 95.1)	144 (139, 149)	345	4.7	560	7.1	58.1[f]
Atorvastatin	300 (244, 355)	311 ± 110	1164	22.0	1210	22.4	35[b]
Bosentan	232 (166, 297)	231 ± 94	900	6.8	899	6.8	23[c]
Glyburide	461 (403, 518)	1587 (1078, 2095)	1790	3.3	6168	9.7	6.8[g]
Asunaprevir	2210 (1759, 2661)	2668 (2454, 2882)	8592	32.7	10373	34.4	38.4[e]
Telmisartan	ND (n=2)	2625 ± 462	ND	ND	10205	26.5	14.6[d]

The $PS_{u,inf}$ data is presented as either mean of 2 independent experiments (individual data are given in parentheses) or mean ± S.D. of 3-5 independent experiments. [a]Data is referenced from (Yamashiro et al. 2006); [b]Data is referenced from (Watanabe et al. 2010); [c]Data is referenced from (Treiber et al. 2004); [d]Data is referenced from (Wolfgang Wienen et al. 2000); [e]Data is referenced from (Mosure et al. 2015); [f]Data is referenced from (Tamura et al. 2010); [g]Data is referenced from (Zhou et al. 2016). ND, not detected.

Table 3. $Kp_{,uu}$ Values Determined in Rat Hepatocytes Using Different Methods

	Temp $Kp_{uu,ss}$		Hom $Kp_{uu,ss}$		$Kp_{uu,V0}$	
Compound	**no BSA**	**w BSA**	**no BSA**	**w BSA**	**no BSA**	**w BSA**
Rosuvastatin	17.1 (13.5, 20.6)	15.4 ± 4.66	12.6 (14.5, 10.7)	19.0 ± 4.52	54.9 (91.6, 18.2)	37.9 ± 11.4
Pravastatin	11.1 (15.8, 6.43)	4.80 (3.90, 5.69)	2.47 (3.84, 1.10)	2.62 (2.82, 2.42)	7.64 (4.88, 10.4)	30.2 (54.5, 5.97)
Valsartan	21.0 ± 14.6	8.43 (12.9, 3.95)	4.70 ± 1.71	96.5 (104, 89)	29.6 ± 15.9	12.8 (11.1, 14.5)
Pitavastatin	15.1 (22.1, 8.15)	11.6 ± 2.38	4.28 (4.10, 4.46)	7.30 ± 3.55	9.06 (6.22, 11.9)	6.33 ± 0.91
Fluvastatin	5.27 (5.42, 5.12)	20.1 (26.4, 13.7)	4.20 (4.90, 3.50)	16.6 (17.4, 15.8)	4.42 (5.60, 3.24)	11.7 (9.40, 13.9)
Cerivastatin	8.62 ± 1.37	5.75 (6.49, 5.0)	8.00 ± 0.71	15.8 (11.8, 19.7)	7.56 ± 0.33	6.25 ± 5.17
Nateglinide	10.8 (11.1, 10.4)	4.90 (6.80, 2.99)	2.27 (2.37, 2.16)	5.30 (4.85, 5.74)	5.22 (4.41, 6.02)	2.09, 2.39
Atorvastatin	10.5 (9.86, 11.2)	11.2 (10.3, 12.1)	4.71 (3.28, 6.14)	9.08 ± 4.01	12.8 (12.8, 12.7)	10.4 ± 5.36
Bosentan	5.51 (5.14, 5.88)	3.90 (3.53, 4.26)	4.38 (3.20, 5.56)	4.64 ± 1.96	6.31 (5.00, 7.62)	8.72± 3.51
Glyburide	6.73 (7.11, 6.35)	17.1 (23.5, 10.6)	2.26 (1.92, 2.60)	16.8 (14.9, 18.6)	19.4 (16.6, 22.2)	94.0 (14.9, 173)
Asunaprevir	5.02 (5.58, 4.45)	10.8 (11.2, 10.4)	0.94 (0.646, 1.24)	1.51 ± 0.11	2.12 (2.67, 1.56)	5.19 (4.24, 6.13)
Telmisartan	2.17 (1.89, 2.45)	4.17 ± 0.72	0.74 (0.647, 0.832)	6.84 ± 1.23	ND (n=2)	35.6 ± 10.0

The data are presented as mean of 2 independent experiments (individual data are given in parentheses) or mean ± S.D. of 3-5 independent experiments; ND, not detected.

Table 4. Predicted Rat Hepatic Clearance based on Extended Clearance Concept: $CL_{int,met}$ x Kp_{uu}

		$CL_{int, met}$		Temp $Kp_{uu,ss}$				Hom $Kp_{uu,ss}$				$Kp_{uu, V0}$			
				no BSA		w BSA		no BSA		w BSA		no BSA		w BSA	
Compound	**Observed Rat CL (mL/min/Kg)[c]**	**Rat Hepatocyte $CL_{int,met}$ (mL/min/Kg)[a]**	**Pred rat CL (ml/min/Kg)**	**CL_{int} (ml/min/kg)**	**Pred rat CL (ml/min/Kg)**	**CL_{int} (ml/min/kg)**	**Pred rat CL (ml/min/Kg)**	**CL_{int} (ml/min/kg)**	**Pred rat CL (ml/min/Kg)**	**CL_{int} (ml/min/kg)**	**Pred rat CL (ml/min/Kg)**	**CL_{int} (ml/min/kg)**	**Pred rat CL (ml/min/Kg)**	**CL_{int} (ml/min/kg)**	**Pred rat CL (ml/min/Kg)**
Rosuvastatin	56.7	77.0	5.23	1706	31.7	1541	30.6	1261	28.5	1901	32.7	5493	40.4	3794	38.3
Pravastatin	59.7	28.5[b]	14.51	373	38.6	161	31.7	83	24.5	88	25.2	257	35.9	1015	43.1
Valsartan	17.8	79.2	0.29	2107	5.4	844	2.3	471	1.3	9669	17.4	2962	7.2	1283	3.4
Pitavastatin	28.0	179	1.99	4848	18.7	3733	15.9	1372	7.5	2341	11.4	2904	13.4	2029	10.3
Fluvastatin	20.0	151	4.04	1557	15.5	5925	30.4	1241	13.3	4906	28.4	1306	13.8	3443	24.4
Cerivastatin	24.7	186	7.64	2719	29.1	1813	24.6	2523	28.3	4970	35.0	2385	27.7	1971	25.6
Nateglinide	58.1	169	3.23	2492	20.7	1135	12.4	525	6.7	1228	13.2	1209	13.0	519	6.7
Atorvastatin	35.0	353	14.04	5900	37.9	6275	38.4	2639	31.1	5089	36.9	7143	39.2	5836	37.9
Bosentan	23.0	153	1.98	1280	9.1	905	6.9	1018	7.6	1079	8.0	1466	10.2	2027	13.0
Glyburide	6.8	212	0.70	2375	4.3	6017	9.5	798	1.5	5911	9.4	6846	10.6	33154	27.2
Asunaprevir	38.4	141	5.24	2280	18.1	4910	26.8	429	5.0	688	7.5	961	9.8	2357	18.4
Telmisartan	14.6	90.6	1.20	437	2.5	840	4.6	149	0.9	1378	7.1	ND	ND	7168	22.5

[a] $CL_{int, met}$ (mL/min/Kg) values was calculated based on the $CL_{int, met}$ (µL/min/10^6cells) list in Table 1 using scaling factor of 108 x10^6 cells/g liver and 36 g liver /Kg body weight.

[b] Determined in rat liver S9 at unit of mL/min/g liver (Watanabe et al. 2009), converted to mL/min/Kg using scaling factor of 36 g liver /Kg body weight.

[C] refer to Table 2.

ND, not detected.

Table 5. Comparison of the CL predictability by the tested IVIVE approaches (Observed: predicted)

	$CL_{int,met}$	$PS_{u,\ inf}$		Temp $Kp_{uu,ss}$		Hom $Kp_{uu,ss}$		$Kp_{uu,\ V0}$	
		no BSA	**w BSA**	**no BSA**	**w BSA**	**no BSA**	**w BSA**	**no BSA**	**w BSA**
Rosuvastatin	10.8	3.3	2.3	1.8	1.8	2.0	1.7	1.4	1.5
Pravastatin	4.1	4.0	3.6	1.5	1.9	2.4	2.4	1.7	1.4
Valsartan	61.6	46.9	3.2	3.3	7.7	13.4	1.0	2.5	5.2
Pitavastatin	14.0	5.1	3.0	1.5	1.8	3.7	2.4	2.1	2.7
Fluvastatin	4.9	1.7	1.2	1.3	1.5	1.5	1.4	1.5	1.2
Cerivastatin	3.2	1.1	1.2	1.2	1.0	1.1	1.4	1.1	1.0
Nateglinide	18.0	12.5	8.2	2.8	4.7	8.6	4.4	4.5	8.7
Atorvastatin	2.5	1.6	1.6	1.1	1.1	1.1	1.1	1.1	1.1
Bosentan	11.6	3.4	3.4	2.5	3.4	3.0	2.9	2.3	1.8
Glyburide	9.8	2.0	1.4	1.6	1.4	4.4	1.4	1.6	4.0
Asunaprevir	7.3	1.2	1.1	2.1	1.4	7.7	5.1	3.9	2.1
Telmisartan	12.2	ND	1.8	5.8	3.2	16.4	2.1	ND	1.5
AAFE	8.99	3.48	2.23	1.95	2.11	3.72	2.00	1.92*	2.11*
RMSLE	0.83	0.58	0.40	0.32	0.37	0.58	0.35	0.32*	0.4*

NA, not available; ND: not detected.

*not included in the inter-experimental variability

DMD Fast Forward. Published on August 5, 2020 as DOI: 10.1124/dmd.120.000064
This article has not been copyedited and formatted. The final version may differ from this version.

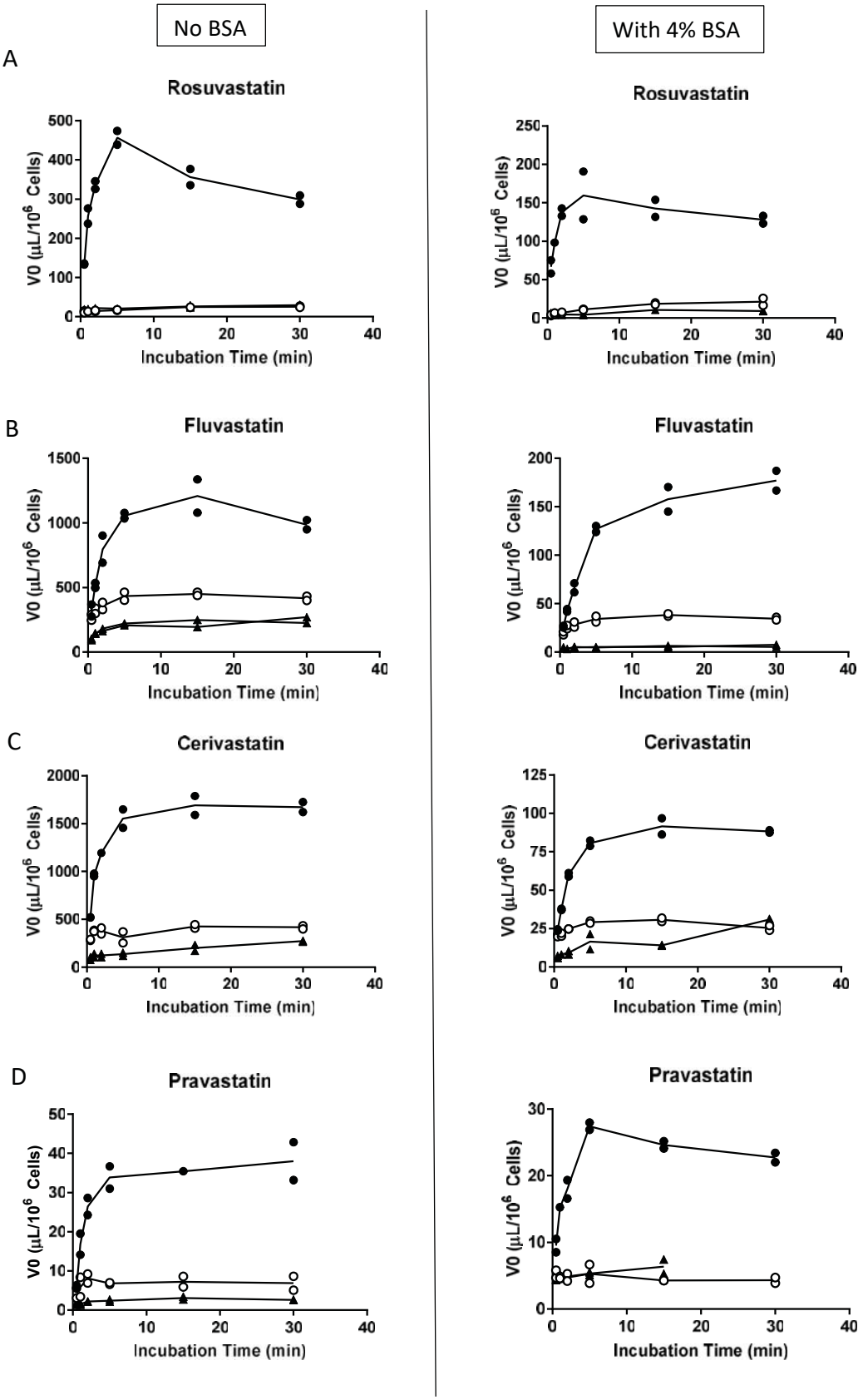

Figure 1.

DMD Fast Forward. Published on August 5, 2020 as DOI: 10.1124/dmd.120.000064
This article has not been copyedited and formatted. The final version may differ from this version.

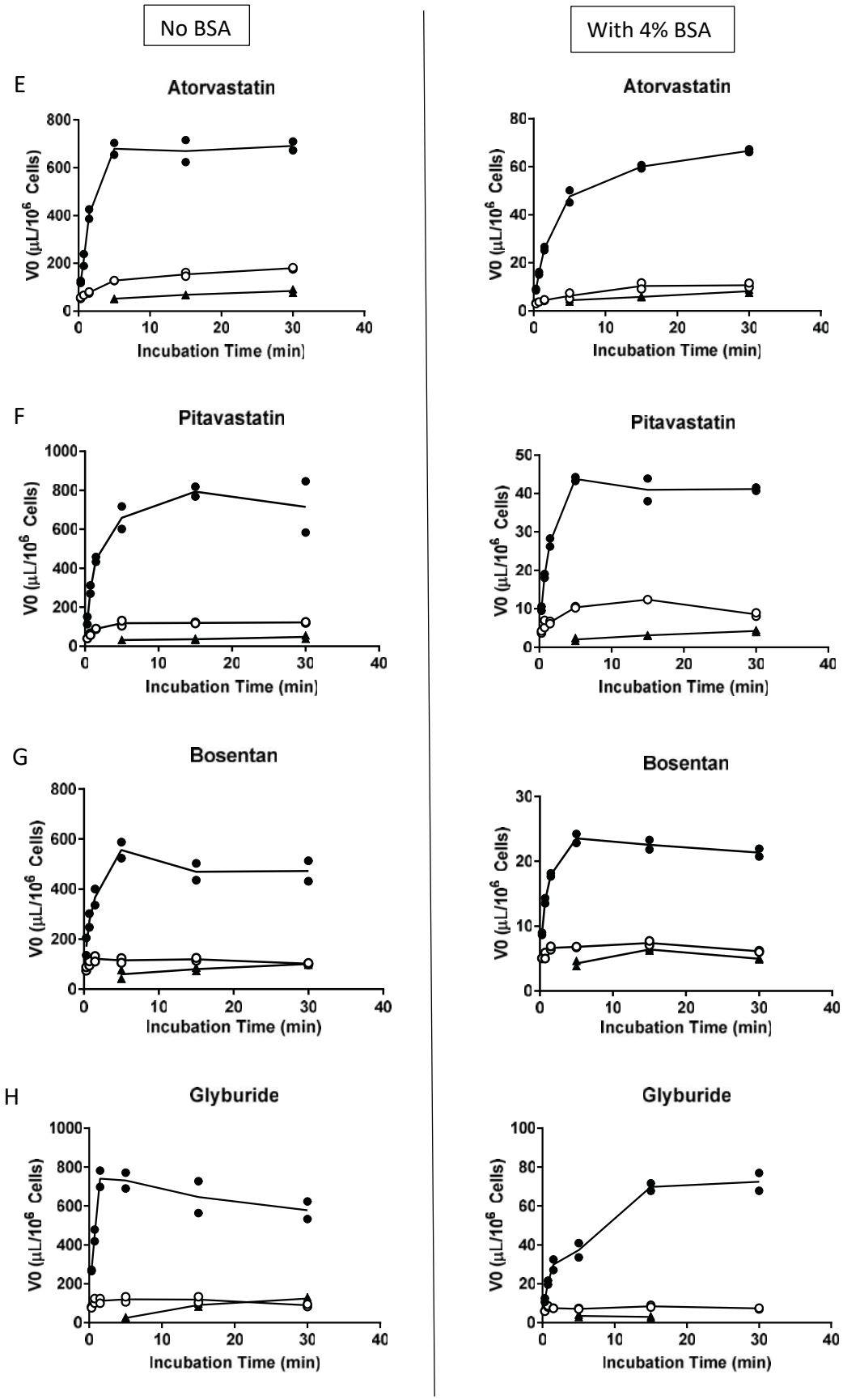

Figure 1. (continue)

DMD Fast Forward. Published on August 5, 2020 as DOI: 10.1124/dmd.120.000064
This article has not been copyedited and formatted. The final version may differ from this version.

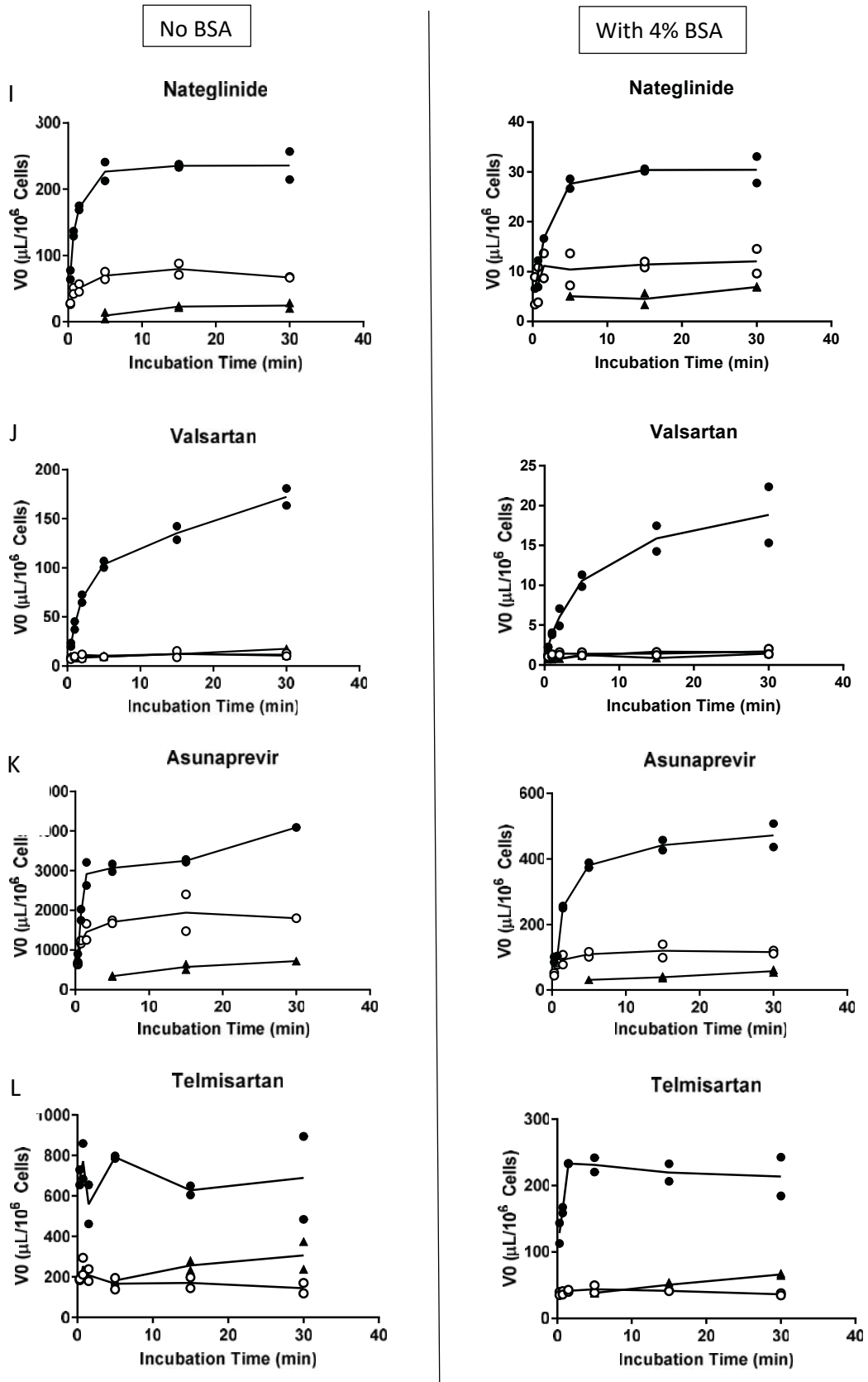

Figure 1. (continue)

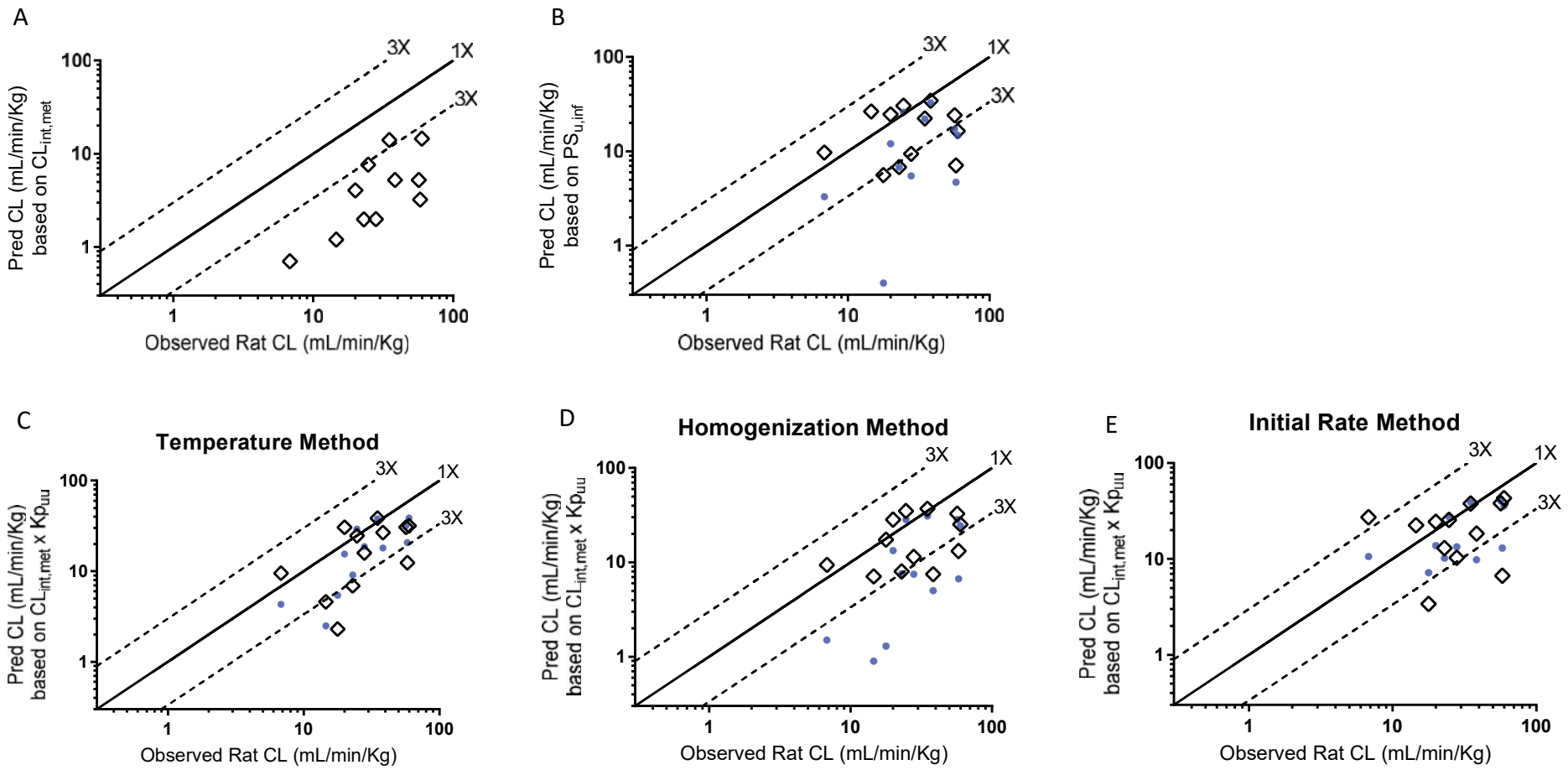

Figure 2.

#DMD-AR-2020-000064

Comparison of In Vitro to In Vivo Extrapolation Approaches for Predicting Transporter-Mediated Hepatic Uptake Clearance Using Suspended Rat Hepatocytes

Na Li, Akshay Badrinarayanan, Xingwen Li, John Roberts, Mike Hayashi, Manpreet Virk,

Anshul Gupta*

Department of Pharmacokinetics and Drug Metabolism, Amgen Research, Amgen Inc. Cambridge, MA 02142

*Corresponding Author: Anshul Gupta

Address: Department of Pharmacokinetics and Drug Metabolism, Amgen Research, Amgen Inc.

360 Binney St., Cambridge, MA 02142

Phone: +1 (617) 444 5205

Email: agupta.pharmaceuticals@gmail.com

Journal: Drug Metabolism and Disposition

The material includes Supplemental Table S1, Supplemental Methods and References.

Supplemental Materials:

Table S1: Summary of the in vitro and in vivo evidence of OATP-mediated hepatic uptake of the selected compounds

	Transporters involved in hepatic uptake			Preclinical and clinical evidence of OATP involvement		
Compound	**Approach**	**Hepatic Transporters**	**Reference**	**Approach**	**PK Change**	**Reference**
Rosuvastatin	RAF and REF	OATP1B1 (M) and OATP1B3 (total 96% and 80%)	(Kunze et al., 2014) [a]	oatp1a/1b KO mice	i.v. : AUC↑ 1.7-fold PO: Cmax ↑ 3-fold; AUC↑ 7.1-fold	(Iusuf et al., 2013)
	RAF	OATP1B1(>95%) and OATP1B3 (<5%)	(Izumi et al., 2018) [b]	oatp1a/1b KO mice	i.v. : AUC↑ 2.3-fold PO: Cmax ↑ 35-fold; AUC↑ 48-fold	(Salphati et al., 2014)
	Hepatocytes with inhibitor	OATP1B1/1B3 (71%), 2B1 (21%) and NTCP (6%)	(Bi et al., 2019)	Clinical DDI with rifampicin (RIF)	+ 600 mg RIF: Cmax ↑ 5.2-fold; AUC↑ 2.5-fold	(Mori et al., 2020)
Pravastatin	RAF and REF	OATP1B1 (M) and OATP1B3 (total 88% and 70%)	(Kunze et al., 2014) [a]	oatp1a/1b KO mice	AUC↑ 4.3-fold	(Higgins et al., 2014)
	RAF	OATP1B1 (>95%) and OATP1B3 (<5%)	(Izumi et al., 2018) [b]	oatp1a/1b KO mice	i.v. AUC↑ 4-fold PO: Cmax ↑ 9.7-fold; AUC↑ 18-fold	(Salphati et al., 2014)
	Hepatocytes with inhibitor	OATP1B1/1B3 (98%)	(Bi et al., 2019)	Clinical DDI with cyclosporin A (CsA)	+ 2x 100 mg CsA: Cmax ↑ 3.2-fold; AUC↑ 3.4-fold	(Yee et al., 2019)
Valsartan	RAF	OATP1B1 (20-70%) and 1B3 (30-80%)	(Yamashiro et al., 2006)	Clinical DDI with RIF	+ 600 mg RIF: Cmax ↑ 3.7-fold; AUC↑ 5.5-fold	(Mori et al., 2020)
	RAF	OATP1B1 (>75%) and 1B3 (<25%)	(Izumi et al., 2018)[b]			
Pitavastatin	RAF	OATP1B1 (90%) and OATP1B3 (10%)	(Hirano et al., 2004)	oatp1a/1b KO mice	PO: Cmax ↑ 13.5-fold; AUC↑ 11.7-fold	(Salphati et al., 2014)
	RAF and REF	OATP1B1 (M) and OATP1B3 (total 43% and 35%)	(Kunze et al., 2014) [a]	oatp1a/1b KO mice	i.v.: AUC↑ 3.7-fold	(Chang et al., 2019)
	RAF	OATP1B1 (>90%) and OATP1B3 (<10%)	(Izumi et al., 2018) [b]	Clinical DDI with RIF	+ 600 mg RIF: Cmax ↑ 3.7-fold; AUC↑ 4.0-fold	(Mori et al., 2020)
	Hepatocytes: inhibitor	OATP1B1/1B3 (81%), 2B1 (12%)	(Bi et al., 2019)			
Fluvastatin	RAF and REF	OATP1B1 (M) and OATP1B3 (total 50% and 42%)	(Kunze et al., 2014) [a]	oatp1a/1b KO mice	i.v.: AUC↑ 1.7-fold	(Chang et al., 2019)
	RAF	OATP1B1 (>93%) and OATP1B3 (<7%)	(Izumi et al., 2018) [b]			
	Hepatocytes: inhibitor	OATP1B1/1B3 (48%), 2B1 (12%) and NTCP (16%)	(Bi et al., 2019)			
Cerivastatin	RAF and REF	OATP1B1 (M) and OATP1B3 (total 19% and 16%)	(Kunze et al., 2014) [a]	Clinical DDI with CsA	AUC↑ 3.8-fold	(Shitara et al., 2013)
	RAF	OATP1B1 (>95%) and OATP1B3 (<5%)	(Izumi et al., 2018) [b]			
Nateglinide	RAF	OATP1B1(>85%) and 1B3 (<15%)	(Izumi et al., 2018) [b]	Clinical DDI with fluconazole	AUC↑ 1.5-fold	(Niemi et al., 2003)
Atorvastatin	RAF and REF	OATP1B1 (M) and OATP1B3 (total 73% and 63%)	(Kunze et al., 2014) [a]	oatp1a/1b KO mice	AUC↑ 19-fold	(Higgins et al., 2014)
	RAF	OATP1B1 (>85%) and 1B3(<15%)	(Izumi et al., 2018) [b]	Clinical DDI with RIF	+ 600 mg RIF: Cmax ↑ 13.3-fold; AUC↑ 7.3-fold	(Mori et al., 2020)
Bosentan	RAF	OATP1B1 (>90%) and 1B3 (<10%)	(Izumi et al., 2018) [b]	Clinical DDI with RIF	+ 600 mg RIF: AUC↑ 3.2-fold	(Yoshikado et al., 2017)
Glyburide	RAF	OATP1B1 (>95%) and 1B3 (<5%)	(Izumi et al., 2018) [b]	Clinical DDI with RIF	+ 600 mg RIF: AUC↑ 2.2-fold	(Shitara et al., 2013)
Asunaprevir	Hepatocytes	Saturable Uptake	(Eley et al., 2015)	Clinical DDI with rifampin	PO: Cmax ↑ 21-fold; AUC↑ 15-fold	(Eley et al., 2015)
Telmisartan	RAF	OATP1B3 only	(Ishiguro et al., 2006)	Clinical DDI with Nisoldipine	AUC↑ 2.3-fold	(Bajcetic et al., 2007)
	RAF	OATP1B3 only	(Izumi et al., 2018) [b]			

[a]In Kunze, et al, the percent contribution of both OATP1B1 and OATP1B3 to the total active hepatic uptake clearance determined using RAF and REF respectively were listed in the parentheses. M in the parentheses indicated the major OATP involved in hepatic uptake.

[b]The percent contribution (%) cited from Izumi, et al and others represents the relative contribution of OATP1B1 and OATP1B3 to hepatic uptake.

RIF: rifampicin

CsA: cyclosporin A

Supplemental methods:

Bioanalysis using RapidFire

Analysis of specimens for intrinsic metabolic CL in rat hepatocytes was performed using the RapidFire 365 high-throughput SPE system interfaced with a 6550 QTOF mass spectrometer with dual Agilent Jet (AJS) ESI source (Agilent Technologies, Santa Clara, CA, USA). The instrument settings were gas temperature at 200°C, drying gas at 18 l/min, nebulizer 40 psig, sheath gas temperature at 350°C, sheath gas flow at 12 l/min and Vcap at 5000 V. The acquisition rate/time was 5 spectra/s and Mass range was 100 to 700 m/z. Specimens were analyzed in positive mode. The load/wash solvent (solvent A) was water containing 0.1% (v/v) formic acid. The elution solvent (solvent B) was acetonitrile containing 0.1% (v/v) formic acid. Specimens were aspirated serially, under vacuum, directly from multi-well assay plates. In each case, a 10 µL aliquot was loaded onto a C18 SPE cartridge (cartridge type A) to remove buffer salts, using solvent A at a flow rate of 1.5 ml/min for 3500 ms. The retained and purified analytes were eluted to the mass spectrometer by washing the cartridge with solvent B at 0.60 to 0.8 ml/min for 3500 ms. The cartridge was re-equilibrated with solvent A for 500 ms at 1.5 ml/min. The entire sampling cycle was around 8 s per well, enabling the analysis of a 96-well plate in approximately 13 min.

LC-MS/MS Quantification

The Shimadzu LC system included two LC-20ADXR pumps, a SIL-30ACMP auto sampler, a CBM-20A controller and a CTO-20A column oven (Shimadzu, USA). The chromatography was performed using C18 column (Cadenza 5CD - C18, 5 µM, 2 X 30mm, Imtakt, USA). Sample injection volume was 5µL and the LC flow rate was 1.2 mL/min. Mobile phase (A) was water with 0.1% formic acid and mobile phase (B) was acetonitrile with 0.1% formic acid. The gradient elution started with a 0.1 min hold at 5% mobile phase (B), followed by a 0.8 min ramp to 95% mobile phase (B) and hold for 0.5 min, followed by a 0.1 min ramp to 5% mobile phase (B) and a hold for 0.4 min re-equilibration. Integrated valco valve was used and the injected liquid was directed into Mass Spectrometer from 0.3 min to 1.8 min. The triple-quadruple instrument is an AB Sciex 5500 QTrap. The mass spectrometer and peripherals were all controlled by Analyst™ (version 1.6.3; AB Sciex, Ontario, Canada) and DiscoveryQuant™

software (version 3.0.1; AB Sciex, Ontario, Canada). Positive ionizations were used in selected reaction monitoring (MRM) scan mode. All the transitions of twelve compounds are listed below.

Compound	MW	Q1	Q3	DP	CE	CPX	EP
Glyburide	494	495.2	370.1	73	10	9	8
Nateglinide	317	318.2	69.1	120	25	13	12
Valsartan	435	436.2	291.1	43	10	13	12
Telmisartan	514	515.0	276.1	162	50	13	2
Atorvastatin	558	559.4	440.3	81	10	16	10
Asunaprevir	747	748.3	648.3	60	27	17	5
Pitavastatin	421	422.5	290.2	96	39	10	10
Bosentan	551	551.8	202.0	154	25	15	2
Rosuvastatin	481	482.0	258.1	76	28	20	10
Cerivastatin	459	460.2	356.3	86	20	12	10
Fluvastatin	411	412.3	224.1	71	30	22	10
Pravastatin	446	447.1	327.4	50	23	30	10

References

Bajcetic M, Benndorf RA, Appel D, Schwedhelm E, Schulze F, Riekhof D, Maas R and Boger RH (2007) Pharmacokinetics of oral doses of telmisartan and nisoldipine, given alone and in combination, in patients with essential hypertension. *J Clin Pharmacol* **47**:295-304.

Bi YA, Costales C, Mathialagan S, West M, Eatemadpour S, Lazzaro S, Tylaska L, Scialis R, Zhang H, Umland J, Kimoto E, Tess DA, Feng B, Tremaine LM, Varma MVS and Rodrigues AD (2019) Quantitative Contribution of Six Major Transporters to the Hepatic Uptake of Drugs: "SLC-Phenotyping" Using Primary Human Hepatocytes. *J Pharmacol Exp Ther* **370**:72-83.

Chang JH, Zhang X, Messick K, Chen YC, Chen E, Cheong J and Ly J (2019) Unremarkable impact of Oatp inhibition on the liver concentration of fluvastatin, lovastatin and pitavastatin in wild-type and Oatp1a/1b knockout mouse. *Xenobiotica* **49**:602-610.

Eley T, Han YH, Huang SP, He B, Li W, Bedford W, Stonier M, Gardiner D, Sims K, Rodrigues AD and Bertz RJ (2015) Organic anion transporting polypeptide-mediated transport of, and inhibition by, asunaprevir, an inhibitor of hepatitis C virus NS3 protease. *Clin Pharmacol Ther* **97**:159-166.

Higgins JW, Bao JQ, Ke AB, Manro JR, Fallon JK, Smith PC and Zamek-Gliszczynski MJ (2014) Utility of Oatp1a/1b-knockout and OATP1B1/3-humanized mice in the study of OATP-mediated pharmacokinetics and tissue distribution: case studies with pravastatin, atorvastatin, simvastatin, and carboxydichlorofluorescein. *Drug Metab Dispos* **42**:182-192.

Hirano M, Maeda K, Shitara Y and Sugiyama Y (2004) Contribution of OATP2 (OATP1B1) and OATP8 (OATP1B3) to the hepatic uptake of pitavastatin in humans. *J Pharmacol Exp Ther* **311**:139-146.

Ishiguro N, Maeda K, Kishimoto W, Saito A, Harada A, Ebner T, Roth W, Igarashi T and Sugiyama Y (2006) Predominant contribution of OATP1B3 to the hepatic uptake of telmisartan, an angiotensin II receptor antagonist, in humans. *Drug Metab Dispos* **34**:1109-1115.

Iusuf D, van Esch A, Hobbs M, Taylor M, Kenworthy KE, van de Steeg E, Wagenaar E and Schinkel AH (2013) Murine Oatp1a/1b uptake transporters control rosuvastatin systemic exposure without affecting its apparent liver exposure. *Mol Pharmacol* **83**:919-929.

Izumi S, Nozaki Y, Kusuhara H, Hotta K, Mochizuki T, Komori T, Maeda K and Sugiyama Y (2018) Relative Activity Factor (RAF)-Based Scaling of Uptake Clearance Mediated by Organic Anion Transporting Polypeptide (OATP) 1B1 and OATP1B3 in Human Hepatocytes. *Mol Pharm* **15**:2277-2288.

Kunze A, Huwyler J, Camenisch G and Poller B (2014) Prediction of organic anion-transporting polypeptide 1B1- and 1B3-mediated hepatic uptake of statins based on transporter protein expression and activity data. *Drug Metab Dispos* **42**:1514-1521.

Mori D, Kimoto E, Rago B, Kondo Y, King-Ahmad A, Ramanathan R, Wood LS, Johnson JG, Le VH, Vourvahis M, David Rodrigues A, Muto C, Furihata K, Sugiyama Y and Kusuhara H (2020) Dose-Dependent Inhibition of OATP1B by Rifampicin in Healthy Volunteers: Comprehensive Evaluation of Candidate Biomarkers and OATP1B Probe Drugs. *Clin Pharmacol Ther* **107**:1004-1013.

Niemi M, Neuvonen M, Juntti-Patinen L, Backman JT and Neuvonen PJ (2003) Effect of fluconazole on the pharmacokinetics and pharmacodynamics of nateglinide. *Clin Pharmacol Ther* **74**:25-31.

Salphati L, Chu X, Chen L, Prasad B, Dallas S, Evers R, Mamaril-Fishman D, Geier EG, Kehler J, Kunta J, Mezler M, Laplanche L, Pang J, Rode A, Soars MG, Unadkat JD, van Waterschoot RA, Yabut J, Schinkel AH and Scheer N (2014) Evaluation of organic anion transporting polypeptide 1B1 and 1B3 humanized mice as a translational model to study the pharmacokinetics of statins. *Drug Metab Dispos* **42**:1301-1313.

Shitara Y, Maeda K, Ikejiri K, Yoshida K, Horie T and Sugiyama Y (2013) Clinical significance of organic anion transporting polypeptides (OATPs) in drug disposition: their roles in hepatic clearance and intestinal absorption. *Biopharm Drug Dispos* **34**:45-78.

Yamashiro W, Maeda K, Hirouchi M, Adachi Y, Hu Z and Sugiyama Y (2006) Involvement of transporters in the hepatic uptake and biliary excretion of valsartan, a selective antagonist of the angiotensin II AT1-receptor, in humans. *Drug Metab Dispos* **34**:1247-1254.

Yee SW, Giacomini MM, Shen H, Humphreys WG, Horng H, Brian W, Lai Y, Kroetz DL and Giacomini KM (2019) Organic Anion Transporter Polypeptide 1B1 Polymorphism Modulates the Extent of Drug-Drug Interaction and Associated Biomarker Levels in Healthy Volunteers. *Clin Transl Sci* **12**:388-399.

Yoshikado T, Maeda K, Furihata S, Terashima H, Nakayama T, Ishigame K, Tsunemoto K, Kusuhara H, Furihata KI and Sugiyama Y (2017) A Clinical Cassette Dosing Study for Evaluating the Contribution of Hepatic OATPs and CYP3A to Drug-Drug Interactions. *Pharm Res* **34**:1570-1583.